JCTC Journal of Chemical Theory and Computation

Article

pubs.acs.org/JCTC

Accurate Spin-State Energetics of Transition Metal Complexes. 1. CCSD(T), CASPT2, and DFT Study of $[M(NCH)_6]^{2+}$ (M = Fe, Co)

Latévi Max Lawson Daku,*[,†] Francesco Aquilante,[‡] Timothy W. Robinson,[§] and Andreas Hauser[†]

[†]Université de Genève, Faculté des Sciences, Quai E. Ansermet 30, CH-1211 Genève 4, Switzerland

[‡]Department of Chemistry - Ångström, The Theoretical Chemistry Programme, Uppsala University, P.O. Box 518, SE-751 20 Uppsala, Sweden

[§]CSCS Swiss National Supercomputing Centre, Via Trevano 131, CH-6900 Lugano, Switzerland

Supporting Information

ABSTRACT: Highly accurate estimates of the high-spin/low-spin energy difference ΔE_{HL}^{el} in the high-spin complexes $[Fe(NCH)_6]^{2+}$ and $[Co(NCH)_6]^{2+}$ have been obtained from the results of CCSD(T) calculations extrapolated to the complete basis set limit. These estimates are shown to be strongly influenced by scalar relativistic effects. They have been used to assess the performances of the CASPT2 method and 30 density functionals of the GGA, meta-GGA, global hybrid, RSH, and double-hybrid types. For the CASPT2 method, the results of the assessment support the proposal [Kepenekian, M.; Robert, V.; Le Guennic, B. *J. Chem. Phys.* **2009**, *131*, 114702] that the ionization potential−electron affinity (IPEA) shift defining the zeroth-order Hamiltonian be raised from its standard value of 0.25 au to 0.50−0.70 au for the determination of ΔE_{HL}^{el} in Fe(II) complexes with a $[FeN_6]$ core. At the DFT level, some of the assessed functionals proved to perform within chemical accuracy ($\pm$350 cm^{-1}) for the spin-state energetics of $[Fe(NCH)_6]^{2+}$, others for that of $[Co(NCH)_6]^{2+}$, but none of them simultaneously for both complexes. As demonstrated through a reparametrization of the CAM-PBE0 range-separated hybrid, which led to a functional that performs within chemical accuracy for the spin-state energetics of both complexes, performing density functionals of broad applicability may be devised by including in their training sets highly accurate data like those reported here for $[Fe(NCH)_6]^{2+}$ and $[Co(NCH)_6]^{2+}$.

1. INTRODUCTION

Transition metal (TM) complexes exhibit many interesting physical and chemical properties, which are dictated by the shapes and relative positions of the potential energy surfaces (PESs) of their low-lying spin states. For instance, (pseudo)-octahedral $3d^4$−$3d^7$ TM complexes can exhibit spin crossover (SCO), that is, the entropy-driven thermal depopulation of their electronic low-spin (LS) ground state in favor of the close-lying high-spin (HS) state. SCO is accompanied by a change of the optical, magnetic, and structural properties of the complexes. Furthermore, light irradiation can also be used to control the SCO equilibrium. The SCO complexes are therefore likely to be used in the design of optical devices for the storage and display of information at the molecular level. As such, they are the subject of numerous multidisciplinary studies.[1−3] A change of spin states also takes place in many reactions of TM complexes, as well as in the chemistry of many metalloproteins and metalloenzymes.[4−6]

The in-depth understanding of SCO and related phenomena or of spin-nonconserving reactions of TM systems relies on the accurate description of the PESs of the corresponding spin-states, at given critical points or along given relevant coordinates. Theoretical methods can in principle be used to obtain an accurate description of these PESs. However, such theoretical studies are seriously undermined by the issues tied to the accurate determination of the energy difference between states of different spin multiplicities.

In the framework of density functional theory (DFT),[7,8] the results are strongly dependent on the exchange-correlation (XC) functional used. Although considerable attention has been paid to this issue,[4,5,9−42] no XC functional has emerged so far as the functional of choice for the evaluation of TM spin-state energetics. Furthermore, there is no guarantee that the accuracy of the DFT results shall improve with the degree of sophistication of the functional. In contrast, in wave function theory (WFT), the accuracy of the results can be systematically improved by resorting to methods that improve the treatment of both static and dynamic correlation effects. However, such methods are limited to systems of small to medium size (~100 atoms at most). And, even in the case of the well-established CASPT2 multireference perturbation (MRPT) method,[43,44] some empiricism turns out to be needed in the definition of the zeroth-order Hamiltonian.[45−47] Such limitations can be overcome by resorting to high-level coupled-cluster (CC) methods.[48,49]

CC methods are the most accurate methods for treating electronic correlation in single-reference systems, and even in their standard formulation, they can also be used to reliably cope with situations of multireference character.[48−50] However, CC calculations are unquestionably computationally *very* demanding. For instance, the CCSD and CCSDT methods have canonical scalings of $O(N^6)$ and $O(N^8)$, respectively, where N is the number of basis functions. Consequently, given that sufficiently large basis sets must be used to obtain accurate

Received: July 11, 2012
Published: September 26, 2012

and physically sound results, elaborate CC calculations can only be performed for relatively small systems, *i.e.*, of up to a few tens of atoms. Despite these restraints on the size of the complexes which can thus be investigated, the theoretical characterization of TM spin-state energetics would greatly benefit from the availability of highly accurate CC reference data.

1. These data could be used for a straightforward and stringent assessment of the performance of the less computationally demanding DFT and WFT methods. Despite being appealing, the calibration of computational methods against experimental data is hampered, in the present case, by the fact that the spin-state energetics of TM complexes can be strongly influenced by their surroundings and, as for SCO complexes, by the fact that the available experimental data may actually correspond to enthalpy differences and thus depend on temperature and pressure.[51−53] The accurate inclusion of environmental, temperature, and pressure effects in the description of a TM system is a challenging task, which the use of very accurate gas-phase *ab initio* reference data would allow to bypass in the assessment process.
2. By including them in relevant training data sets, they could serve to develop improved semiempirical density functionals.

In addition, they can be used to predict within DFT the spin-state energetics in complexes of a given TM ion, based on a recent study, which showed that, despite their limitations, DFT methods can be applied to the accurate determination of the spin-state energetics in families of complexes of a TM ion, provided that the spin-state energetics in a reference complex of a given family are accurately known.[54]

Consequently, with the aim to contribute to a comprehensive set of benchmark data, we have undertaken the accurate characterization of the spin-state energetics in TM complexes of inorganic and bioinorganic interests, using high-level CC methods. In this study, we report the results obtained for the HS−LS energy differences in the $3d^6$ iron(II) HS complex $[Fe(NCH)_6]^{2+}$,[9,55,56] and in the hypothetical $3d^7$ cobalt(II) $[Co(NCH)_6]^{2+}$ complex, which have the "MN_6" (M = Fe, Co) first coordination sphere present in the majority of Fe(II) and Co(II) SCO complexes. Their spin-state energy differences have been calculated with the CCSD(T) method,[57] which is considered the gold standard of quantum chemistry, and which is characterized by an $O(N^6)$ scaling for the iterative CCSD part and an $O(N^7)$ scaling for the perturbative connected triples. Sequences of very large basis sets were used and the results extrapolated to the complete basis set (CBS) limit. Scalar relativistic (SR) effects were also taken into account. The highly accurate CC results thus obtained for the spin-state energetics in the $[Fe(NCH)_6]^{2+}$ and $[Co(NCH)_6]^{2+}$ complexes were then used to assess the performances of the CASPT2 method and of the 30 XC energy functionals given in Table 1.

2. COMPUTATIONAL DETAILS

Reference $[M(NCH)_6]^{2+}$ Geometries (M = Fe, Co). The geometries of $[Fe(NCH)_6]^{2+}$ and $[Co(NCH)_6]^{2+}$ used for the CCSD(T), CASPT2, and DFT calculations have been obtained by nonrelativistic (NR) DFT optimizations performed with the ADF program package.[92−94] These DFT calculations were carried out with the OLYP functional[63,71] and the TZP basis set of triple-ζ polarized quality from the ADF Slater-type orbital (STO) basis set database.[95] The Cartesian coordinates of these reference structures are available as Supporting Information (SI).

Table 1. Exchange-Correlation Energy Functionals Used for the DFT Calculations

GGAs	hybrid GGAs
PBE[58,59]	B3LYP[60,61]
BLYP[62,63]	B3LYP*[11]
BP86[62,64,65]	X3LYP[66]
BOP[62,67]	PBE0[68,69]
PBEOP[58,59,67]	B97[70]
OLYP[63,71]	B97-3[72]
OPBE[58,59,71]	B98[73]
HCTCH/407[74]	mPW1K[75]
HCTCH/407+[76]	
meta-GGAs	**hybrid meta-GGAs**
TPSS[77]	BB1K[78]
PKZB[79,80]	TPSSh[81]
M06-L[82]	M05[83,84]
	M06[85]
range-separated hybrids	**double hybrids**
CAM-B3LYP[86]	B2-PLYP[87,88]
LC-BLYP[89,90]	mPW2-PLYP[87,88]
LC-PBE[89,90]	
CAM-PBE0[91]	

CCSD(T) Calculations on $[M(NCH)_6]^{2+}$ (M = Fe, Co). The CC calculations have been performed with the Tensor Contraction Engine (TCE) module[96−98] of the NWChem program package (version 6.0).[99,100] They have been run nonrelativistically and also with scalar relativistic (SR) effects taken into account through the use of the second-order Douglas−Kroll−Hess (DKH or DK) method,[101−103] as implemented in NWChem.[104] The NR CC calculations have been carried out with two series of spherical basis sets, hereafter denoted $S_1^{NR} = \{S_{1,n}^{NR}\}_{n=T,Q}$ and $S_2^{NR} = \{S_{2,n}^{NR}\}_{n=T,Q,5}$, wherein the H, C, and N atoms are described by Dunning's correlation-consistent basis sets,[105] and the TMs by correlation-consistent basis sets of Balabanov and Peterson designed for the accurate treatment of the 3s3p semicore plus valence correlation.[106] The $S_{1,n}^{NR}$ and $S_{2,n}^{NR}$ basis sets are defined by the following combinations of correlation-consistent basis sets (M = Fe or Co):

$$S_{1,n}^{NR} = \{\text{H.cc-pVDZ, C.cc-pV}n\text{Z, N.cc-pV}n\text{Z, M.cc-pwCV}n\text{Z}\} \quad (n = \text{T, Q}) \tag{1}$$

and

$$S_{2,n}^{NR} = \{\text{H.cc-pVDZ, C.cc-pVTZ, N.cc-pVTZ, M.cc-pwCV}n\text{Z}\} \quad (n = \text{T, Q, 5}) \tag{2}$$

We have thus chosen to describe the peripheral H atoms in all these basis sets with the cc-pVDZ basis set. In the $S_{1,n}^{NR}$ series, n is the cardinal number of the correlation-consistent basis sets used to describe the N, C, and TM atoms, and because of the rapid increase of the number of basis functions, we have had to limit n to T and Q. In the $S_{2,n}^{NR}$ series, the N and C atoms are described by the large cc-pVTZ basis set, and n is the cardinal number of the correlation-consistent basis sets used for the TM atoms, taking values in T, Q, and 5. The basis sets $S_{1,T}^{NR}$ and $S_{2,T}^{NR}$ are identical; therefore, starting from a common point, the $S_{1,n}^{NR}$

and $S_{2,n}^{NR}$ sequences provide two different ways for exploring the convergence with respect to the basis sets of the energy differences of interest. In order to determine the SR shifts to these quantities, the DKH CC calculations have been performed with the sequence of spherical basis sets $S_2^{DK} = \{S_{2,n}^{DK}\}_{n=T,Q}$. This series is the DKH counterpart of the S_2^{NR} series in that the correlation consistent basis sets intervening in the definition of $S_{2,n}^{DK}$ have been obtained by recontracting the NR ones used in $S_{2,n}^{NR}$ with the DKH Hamiltonian:[104,106]

$$S_{2,n}^{DK} = \{\text{H.cc-pVDZ-DK, C.cc-pVTZ-DK, N.cc-pVTZ-DK,}$$
$$\text{M.cc-pwCV}n\text{Z-DK}\}\ (n = \text{T, Q}) \quad (3)$$

The characteristics of the $S_{1,n}^{NR}$, $S_{2,n}^{NR}$, and $S_{2,n}^{DK}$ basis sets are summarized in Table 2. This includes the correlation-consistent basis sets used for the different atoms, the corresponding number of contracted functions, and the total number N of basis functions.

Table 2. Definitions of the Series $S_{1,n}^{NR}$, $S_{2,n}^{NR}$, and $S_{2,n}^{DK}$ of Spherical Basis Sets Used in the CCSD(T) Calculations on $[Fe(NCH)_6]^{2+}$ and $[Co(NCH)_6]^{2+}$: Correlation-Consistent Basis Sets Used for the Different Atoms, Corresponding Number of Contracted Functions (in Brackets), and Total Number N of Basis Functions

	H	N, C	Fe, Co	N
		NR $S_{1,n}^{NR}$ basis sets (n = T, Q)		
$S_{1,T}^{NR}$	cc-pVDZ [2s1p]	cc-pVTZ [4s3p2dlf]	cc-pwCVTZ [9s8p6d3f2g]	492
$S_{1,Q}^{NR}$	cc-pVDZ [2s1p]	cc-pVQZ [5s4p3d2f1g]	cc-pwCVQZ [10s9p7d4f3g2h]	839
		NR $S_{2,n}^{NR}$ basis sets (n = T, Q, 5)		
$S_{2,T}^{NR}$	cc-pVDZ [2s1p]	cc-pVTZ [4s3p2d1f]	cc-pwCVTZ [9s8p6d3f2g]	492
$S_{2,Q}^{NR}$	cc-pVDZ [2s1p]	cc-pVTZ [4s3p2d1f]	cc-pwCVQZ [10s9p7d4f3g2h]	539
$S_{2,5}^{NR}$	cc-pVDZ [2slp]	cc-pVTZ [4s3p2dlf]	cc-pwCV5Z [11s10p8d5f4g3h2i]	601
		DKH $S_{2,n}^{DK}$ basis sets (n = T, Q)		
$S_{2,T}^{DK}$	cc-pVDZ-DK [2s1p]	cc-pVTZ-DK [4s3p2d1f]	cc-pwCVTZ-DK [9s8p6d3f2g]	492
$S_{2,Q}^{DK}$	cc-pVDZ-DK [2s1p]	cc-pVTZ-DK [4s3p2d1f]	cc-pwCVQZ-DK [10s9p7d4f3g2h]	539

Using the sequences of basis sets $\{S_{1,n}^{NR}\}_{n=T,Q}$, $\{S_{2,n}^{NR}\}_{n=T,Q,5}$, and $\{S_{2,n}^{DK}\}_{n=T,Q}$, we have estimated the complete basis set (CBS) limits of the quantities of interest by extrapolating the total energies with a two-point l^{-3} formula[107]

$$E_X = E_{CBS} + \frac{A}{X^3} \quad (4)$$

and a mixed exponential and Gaussian formula[108]

$$E_X = E_{CBS} + A' e^{-(X-1)} + B' e^{-(X-1)^2} \quad (5)$$

In the above extrapolation formulas, X = 3, 4, 5, ... for n = T, Q, 5, ... For the CC calculations on the closed-shell LS $[Fe(NCH)_6]^{2+}$ complex, we have used a restricted HF (RHF) reference determinant. The CC calculations on the open-shell species (*i.e.*, $[Fe(NCH)_6]^{2+}$ in the HS state and $[Co(NCH)_6]^{2+}$ in both spin-states) have been performed in the unrestricted framework (UCC calculations). For the NR UCC calculations, a restricted open-shell HF (ROHF) reference wave function has been employed (ROHF-UCC calculations), and as required with the use of a ROHF reference determinant, the Fock matrix was systematically reconstructed in order to obtain correct correlation energies. However, in its current state of development, the TCE module of NWChem cannot reconstruct the Fock matrix when SR effects are operative. Consequently, for performing the DKH UCC calculations, we have used a relativistic unrestricted HF (UHF) reference determinant (UHF-UCC calculations). In order to probe the influence of the choice of the reference wave function on our results, the NR UCC calculations on the open-shell species have also been performed with a UHF reference, using the NR basis sets $S_{2,n}^{NR}$ (n = T, Q). The NR ROHF-UCCSD/$S_{2,n}^{NR}$ and UHF-UCCSD/$S_{2,n}^{NR}$ results (n = T, Q) proved to be very similar, thus reflecting the insensitivity of CCSD to the choice of the reference function.[48] With the full inclusion of higher excitations (CCSDT, CCSDTQ, ...), the CC method becomes further insensitive to the choice of the reference determinant and approaches the invariance of the FCI method.[48] Hence, the perturbative (T) treatment of the connected triples in CCSD(T) explains the dependency on the reference determinant which we have observed for our NR UCCSD(T) results. Interestingly, the differences between the NR ROHF-UCCSD(T) and UHF-UCCSD(T) results are well below the chemical accuracy of 1 kcal/mol ≈ 350 cm^{-1} (see Supporting Information for a comparison of the NR ROHF-UCC and UHF-UCC energy differences determined for $[Fe(NCH)_6]^{2+}$ and $[Co(NCH)_6]^{2+}$). Furthermore, if we denote $\Delta^{SR}(Q)_{\mathcal{M},n}$ the SR shift to a quantity Q determined with the method $\mathcal{M}$ as the difference between the DKH ($Q|_{DK\text{-}\mathcal{M}/S_{2,n}^{DK}}$) and NR ($Q|_{NR\text{-}\mathcal{M}/S_{2,n}^{NR}}$) values of Q:

$$\Delta^{SR}(Q)_{\mathcal{M},n} = Q|_{DK\text{-}\mathcal{M}/S_{2,n}^{DK}} - Q|_{NR-\mathcal{M}/S_{2,n}^{NR}} \quad (6)$$

it turns out that $\Delta^{SR}(Q)_{UCCSD,n} \approx \Delta^{SR}(Q)_{UCCSD(T),n}$ for all the energy differences "Q" of interest to us. That is, the use of an ROHF or UHF reference has a very weak influence on the CCSD(T) determination of the SR shifts to these energy differences, which actually are already quite accurately determined at the HF level (see below). Consequently, within the framework of our CC study based on the use of ROHF references for the open-shell species, accurate DKH CC energy differences are obtained by summing the NR energy differences calculated within this framework and the SR shifts determined by the UHF-UCC calculations.

Table 3. ANO Basis Sets ANO-I and ANO-II Used in the CASSCF and CASPT2 Calculations on the $[M(NCH)_6]^{2+}$ Complexes (M = Fe, Co): Number of Contracted Functions and Total Number N of Basis Functions

	H	C	N	M	N $[M(NCH)_6]^{2+}$
ANO-I	[2slp]	[4s3p2dlf]	[4s3p2dlf]	[7s6p5d3f2glh]	490
ANO-II	[2slp]	[4s3p2dlf]	[5s4p3d2flg]	[10s9p8d6f4g2h]	717

In the remaining text, we will no more mention the nature of the reference determinants used for the CC calculations, which all have been performed in D_{2h}, and wherein all electrons have been correlated. A total of 108 and of 109 electrons have thus been correlated in the CC calculations carried out on $[Fe(NCH)_6]^{2+}$ and $[Co(NCH)_6]^{2+}$, respectively.

CASPT2 Calculations. The CASSCF[109,110] and CASPT2[43,44,111,112] calculations have been performed with a development version of the MOLCAS package[113−115] using the DKH Hamiltonian and two atomic natural orbital (ANO) basis sets. In these basis sets, hereafter denoted ANO-I and ANO-II, all atoms are described with the relativistic ANO-RCC basis sets of Roos and co-workers.[116−118] The contractions of the basis set are given in Table 3 along with the total number of basis functions. In all calculations, the Cholesky decomposition technique for approximating the two-electron integrals was employed.[119] For the CASPT2 calculations, an imaginary shift of 0.1 au was used to avoid intruder states,[120] while the ionization potential−electron affinity (IPEA) shift defining the zeroth-order Hamiltonian[45] was varied between 0 and 2.5 au by steps of 0.05 au.

For the CASSCF calculations on the Fe(II) and Co(II) complexes, we used an active space consisting of six or seven electrons in the five Fe(3d) or Co(3d) orbitals, a second 3d′ shell to account for the double-shell effect,[121] and two doubly occupied metal−ligand σ-bonding orbitals to account for nondynamic correlation effects associated with the covalent metal−ligand interactions.[122] In the course of the CASSCF study of the complexes, it proved necessary to include the 3s semicore orbital and a correlating 3s′ orbital. These orbitals indeed tend to systematically rotate into the active space when the calculations are performed on the geometries of D_{2h} symmetry; this probably follows from the fact that, in D_{2h}, these orbitals can mix with the $3d_{z^2}$ and $3d_{x^2-y^2}$ orbitals. To make the calculations on the $[M(NCH)_6]^{2+}$ complexes (M = Fe, Co) comparable, we have included the 3s and 3s′ orbitals in the active spaces used in all calculations. This especially implies that the CASPT2 calculations correlate the M(3s) semicore orbital along with the M(3p) orbitals which are correlated by default. In summary, (*i*) we have employed for the CASSCF calculations on the Fe(II) and Co(II) complexes a CAS(12,14) and a CAS(13,14) active space, respectively, and (*ii*) for the CASPT2 calculations on both complexes, all valence electrons and the TM semicore 3s and 3p electrons were correlated while the core electrons (C, N: 1s; Co, Fe: 1s, 2s, 2p) were kept frozen.

DFT Calculations. They were performed with the DFT module of the NWChem program package (version 6.0).[99,100] SR effects were not included in the DFT calculations since the SR shifts to the energy differences of interest proved to be already quite well described at the HF level. That is, we expect the determination of the SR shifts within DFT to not be an issue. This was confirmed by the results of test DKH SR calculations performed on $[Co(NCH)_6]^{2+}$ at the PBE/$S^{DK}_{2,Q}$ level (see Supporting Information).

Given the large basis sets used for the calculations, we expect the basis set dependency of the NR results obtained with the non-double-hybrid functionals to be vanishing. This has been validated by the results of a series of test calculations performed with the PBE functional and the $\{S^{NR}_{2,n}\}_{n=T,Q,5}$ basis sets, which indeed showed a very weak dependence on the basis set (see Supporting Information). We have therefore chosen to use the $S^{NR}_{2,Q}$ basis set to perform the calculations with the non-double-hybrid functionals.

Double-hybrid functionals are characterized by the inclusion of a second-order Møller−Plesset (MP2) type perturbation theory correlation contribution.[87] This makes the results obtained with these functionals sensitive to the basis set used. Consequently, the calculations with the B2-PLYP and mPW2-PLYP double-hybrid functionals were performed with the $\{S^{NR}_{2,n}\}_{n=T,Q,5}$ series of basis sets and the results extrapolated to the CBS limit (see Supporting Information). The results reported in the manuscript for the double-hybrid functionals correspond to these CBS values.

3. RESULTS AND DISCUSSION

3.1. CCSD(T) Benchmark Results for $[M(NCH)_6]^{2+}$ (M = Fe, Co). *3.1.1. The Energy Differences of Interest.* We are interested in determining highly accurate values for the HS−LS electronic energy difference ΔE^{el}_{HL} in $[Fe(NCH)_6]^{2+}$ and in $[Co(NCH)_6]^{2+}$, defined by

$$\Delta E^{el}_{HL} = E^{el}_{HS} - E^{el}_{LS} \quad (7)$$

where E^{el}_{HS} and E^{el}_{LS} are the electronic energies of the considered complex in the HS and LS states, respectively.

For the octahedral d^6 complexes such as O_h Fe(II) complexes, the LS and HS states correspond to the ligand-field $^1A_{1g}(t^6_{2g})$ and HS $^5T_{2g}(t^4_{2g}e^2_g)$ states. The nondegenerate $^1A_{1g}(t^6_{2g})$ state can be directly characterized within the single-reference framework of our CC study, not so for the $^5T_{2g}(t^4_{2g}e^2_g)$ state. $[Fe(NCH)_6]^{2+}$ was thus studied in the LS state by performing the calculations on its optimized LS geometry of O_h symmetry (see Supporting Information), and obviously $E^{el}_{LS} = E^{el}(^1A_{1g})$. For $[Fe(NCH)_6]^{2+}$ in the HS state, the optimization of its geometry in D_{2h} led to a minimum which was found to be associated with the $^5B_{2g}$ tetragonal component of the HS state. Indeed, upon the $O_h \rightarrow D_{2h}$ symmetry lowering, the Jahn−Teller (JT) unstable HS state is split according to $^5T_{2g} \rightarrow {}^5B_{1g} \oplus {}^5B_{2g} \oplus {}^5B_{3g}$. Because of the symmetry of the problem, the minima associated with the three tetragonal components are equivalent, and the located $^5B_{2g}$ minimum is representative of all three as they are related by permutations of the ligands located on the principal C_2 axes. The CC calculations were performed for the $^5B_{2g}$ state at the optimized HS geometry. That is, $E^{el}_{HS} = E^{el}(^5B_{2g})$ in eq 7. The choice of the $^5B_{2g}$ HS component for defining E^{el}_{HS} proves to be irrelevant: additional CC calculations performed for determining the energies of the two other HS states at the optimized HS geometry showed that the differences between their energies are tiny (see Supporting Information). The near degeneracy of the three components of the HS state is due to the fact that going from one component to the other mainly involves an electronic rearrangement within the metallic molecular orbitals (MOs) of nonbonding Fe(t_{2g}) parentage. These results suggest that the JT effects in the $^5T_{2g}$ state are rather weak (see Supporting Information).

For the octahedral d^7 complexes such as O_h Co(II) complexes, the LS and HS states correspond to the ligand-field $^2E_g(t^6_{2g}e^1_g)$ and $^4T_{1g}(t^5_{2g}e^2_g)$ states, respectively. Both ligand-field states are degenerate. For the CC study of $[Co(NCH)_6]^{2+}$, we have performed the calculations on optimized D_{2h} LS and HS geometries. Upon the $O_h \rightarrow D_{2h}$ symmetry lowering, the HS state is split into three components, $^4T_{1g} \rightarrow {}^4B_{1g} \oplus {}^4B_{2g} \oplus {}^4B_{3g}$. The optimization led to the location of the minimum

Table 4. NR and DKH Results Obtained at the HF, CCSD, and CCSD(T) Levels for the HS−LS Energy Difference ΔE^{el}_{HL} (cm^{-1}) in $[M(NCH)_6]^{2+}$ (M = Fe, Co)

	$[Fe(NCH)_6]^{2+}$			$[Co(NCH)_6]^{2+}$		
	HF	CCSD	CCSD(T)	HF	CCSD	CCSD(T)
NR results, $S^{NR}_{1,n}$ (n = T, Q) basis sets						
$S^{NR}_{1,T}$	−32535	−8808	−4388	−18789	−7008	−5018
$S^{NR}_{1,Q}$	−32692	−7825	−3186	−18848	−6469	−4363
$S^{NR}_{1,\infty}$ [a]	−32806	−7108	−2309	−18890	−6076	−3885
NR results, $S^{NR}_{2,n}$ (n = T, Q, 5) basis sets						
$S^{NR}_{2,T} \equiv S^{NR}_{1,T}$	−32535	−8808	−4388	−18789	−7008	−5018
$S^{NR}_{2,Q}$	−32492	−7636	−3071	−18765	−6398	−4325
$S^{NR}_{2,5}$	−32534	−6944	−2294	−18779	−6069	−3956
$S^{NR}_{2,\infty}$ (TQ) [b]	−32461	−6780	−2111	−18747	−5953	−3819
$S^{NR}_{2,\infty}$ [c]	−32558	−6539	−1838	−18788	−5876	−3739
SR shifts $\Delta^{SR}(\Delta E^{el}_{HL})_{\mathcal{M},n}$ (n = T, Q) as given by eq 6						
n = T	1337	1359	1384	757	719	723
n = Q	1336	1326	1349	757	704	706
$n = \infty$ [d]	1336	1301	1324	757	692	694

[a]CBS values obtained with the $S^{NR}_{1,n}$ (n = T, Q) results and eq 4. [b]CBS values obtained with the $S^{NR}_{2,n}$ (n = T, Q) results and eq 4. [c]CBS values obtained with the $S^{NR}_{2,n}$ (n = T, Q, 5) results and eq 5. [d]CBS values obtained with the n = T and n = Q results and eq 4.

associated with the $^4B_{1g}$ HS state. As explained above for $[Fe(NCH)_6]^{2+}$ in the HS state, this relaxed HS geometry of $[Co(NCH)_6]^{2+}$ is representative of the minima associated with the three tetragonal components of the HS $^4T_{1g}$ state. The CC calculations have been performed on this HS geometry with the purpose of determining the energy of the $^4B_{1g}$ HS state. Hence, $E^{el}_{HS} = E^{el}(^4B_{1g})$ in eq 7. The choice of the $^4B_{1g}$ state for the definition of E^{el}_{HS} should to be irrelevant because going from one component of the $^4T_{1g}$ state to the other mainly involves an electronic rearrangement within the MOs of nonbonding Co(t_{2g}) parentage. For the same reason, the JT effects of the HS $^4T_{1g}$ state should be weak (see Supporting Information). This should not be the case for the LS $^2E_g(t^6_{2g}e^1_g)$ state because the JT instability results from the single occupancy of the degenerate metallic MOs of antibonding Co(e_g) character. Upon the $O_h \rightarrow D_{2h}$ symmetry lowering, the ^2E_g state gets split into two ^2A_g states. The geometry optimization led to the location of a ^2A_g minimum and a ^2A_g saddle point. The saddle point is characterized by a vibrational mode of imaginary frequency and of a_g symmetry which transforms the geometry at the saddle point to the geometry at the minimum. So, the saddle point is a transition state between two such minima. Due to the tetragonal symmetry of the JT problem, there are actually three equivalent ^2A_g minima and three associated equivalent ^2A_g saddle points. The presence of the saddle points indicates that quadratic vibronic coupling is effective, and if the JT instability of the LS state can be well described by an ideal single-mode E ⊗ e problem, the section of the LS potential energy surface (PES) along the effective e mode would resemble the warped Mexican hat potential.[123] For the determination of ΔE^{el}_{HL} in $[Co(NCH)_6]^{2+}$, the energy of the ^2A_g minimum is used as the energy of the LS state: $E^{el}_{LS} = E^{el}(^2A_g; \text{min})$. CC calculations were also carried out for evaluating the energy $E^{el}(^2A_g; \text{sad})$ of the saddle point and consequently the height Δ_{JT} of the barrier between the LS minima

$$\Delta_{JT} = E^{el}(^2A_g; \text{sad}) - E^{el}(^2A_g; \text{min}) \quad (8)$$

which is also the height of the barrier to pseudorotation, that is, to the rotation of the JT distortions between the equivalent minima on the lowest sheet of the LS PES.[124,125] Although it will only be considered in the CASPT2 study of $[Co(NCH)_6]^{2+}$, we also define here the JT stabilization energy of LS $[Co(NCH)_6]^{2+}$:

$$E_{JT} = E^{el}(^2E_g) - E^{el}(^2A_g; \text{min}) \quad (9)$$

The reliability of the CCSD(T) results depends on the fact that the studied electronic states do not exhibit a strong multireference character due to electronic near degeneracy. The obtention in the CCSD calculations of T_1 and T_2 excitation amplitudes significantly larger in magnitude than 0.1 is considered as being indicative of such an unfavorable situation of significant nondynamical correlation effects (see, for instance, ref 126). In our case, the calculated T_1 and T_2 amplitudes are smaller than 0.1 (the five largest T_1 and T_2 amplitudes for the NR CCSD/$S^{NR}_{2,Q}$ are given in the Supporting Information): this makes us confident about the quality of the results of our single-reference CCSD(T) calculations. We must however mention that there is currently no definitive diagnostic based on CC results for the identification of situations of significant multireference character. Jiang et al.[127] have recently analyzed for various first-row TM species several diagnostics, among them the widely used $\mathcal{T}_1$ and $\mathcal{D}_1$ diagnostics,[128−131] as well as the percentage %TAE of the perturbative triple contribution to the total atomization energy.[132,133] They found that the usual criteria $\mathcal{T}_1 > 0.02$ and $\mathcal{D}_1 > 0.05$ of multireference character derived from the studies of main group species are not well suited for the 3d TM species in that the thresholds used should be increased. Their detailed analysis thus led them to suggest three new criteria for substantial multireference character in 3d TM species; namely, $\mathcal{T}_1 > 0.05$ and $\mathcal{D}_1 > 0.15$ and |%TAE| > 10.[127] However, as they pointed out, the disregard of one or more of these criteria does not imply that the electronic structure has a single-reference or a weak multireference character. Nevertheless, the weight of the leading configuration in a CASSCF wave function proved to remain a useful diagnostic, provided that the active space includes all critical molecular orbitals. This is the case for the active spaces used in our CASSCF calculations, and effectively, the weak multireference character of the electronic states

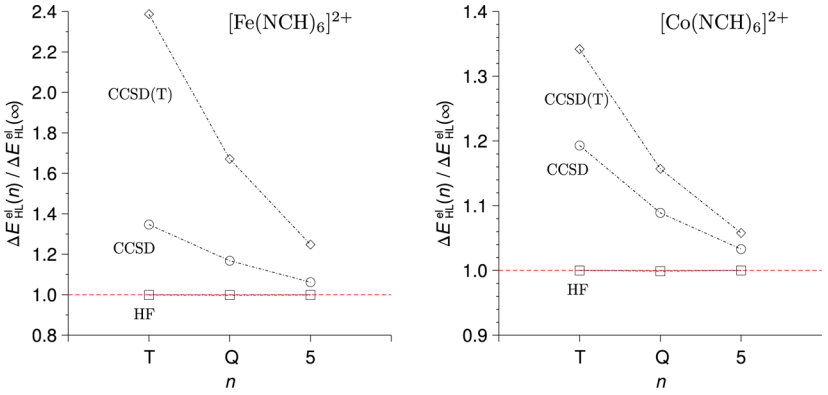

Figure 1. Convergence with respect to the basis set of the calculated HF (□), CCSD (○), and CCSD(T) (◊) values of ΔE_{HL}^{el} in $[Fe(NCH)_6]^{2+}$ and in $[Co(NCH)_6]^{2+}$, in the case where the sequence of basis sets $\{S_{2,n}^{NR}\}_{n=T,Q,5}$ has been used: Plots of the ratios of the calculated energy differences $\Delta E_{HL}^{el}|_{\mathcal{M}/S_{2,n}^{NR}} = \Delta E_{HL}^{el}(n)$ to their CBS values $\Delta E_{HL}^{el}|_{\mathcal{M}/S_{2,\infty}^{NR}} = \Delta E_{HL}^{el}(\infty)$ ($\mathcal{M}$ = HF, CC, CCSD(T); lines serve as guide to the eye).

studied by the CCSD(T) method is also observed in the CASSCF wave functions (see below).

In the following, we will first discuss the NR results obtained for the energy differences ΔE_{HL}^{el} and Δ_{JT} (section 3.1.2), before discussing the influence of SR effects (section 3.1.3).

3.1.2. NR Results. HS−LS Energy Differences in $[M(NCH)_6]^{2+}$ (M = Fe, Co). The results obtained for the HS−LS energy difference ΔE_{HL}^{el} in $[Fe(NCH)_6]^{2+}$ and in $[Co(NCH)_6]^{2+}$ are summarized in Table 4. They include the HF, CCSD, and CCSD(T) values of ΔE_{HL}^{el} calculated with the different sequences of basis sets $[S_{1,n}^{NR}$ (n = T, Q) and $S_{2,n}^{NR}$ (n = T, Q, 5)] as well as the extrapolated CBS values. For both complexes, one notes in Table 4 that, irrespective of the basis set used and in the CBS limit also, the calculated ΔE_{HL}^{el} values increase with the degree of treatment of electronic correlation as follows

$$\Delta E_{HL}^{el}|_{HF} \ll \Delta E_{HL}^{el}|_{CCSD} < \Delta E_{HL}^{el}|_{CCSD(T)} < 0 \qquad (10)$$

For either of the $[M(NCH)_6]^{2+}$ complexes (M = Fe, Co), owing to the fact that the number of paired electrons in the compact 3d shell is larger in the LS state than in the HS state, the electronic correlation is far more important in the LS state than in the HS state. The strong overestimation of the stability of the HS state with respect to the LS state at the uncorrelated HF level is due to the lack of correlation treatment. The situation markedly improves on going from the HF to the CCSD level. However, the HS-LS differential correlation energy is still severely underestimated by the CCSD method. The increase of ΔE_{HL}^{el} brought about by the perturbative triples (T) is on the order of 4500 cm^{-1} and 2000 cm^{-1} for $[Fe(NCH)_6]^{2+}$ and $[Co(NCH)_6]^{2+}$, respectively.

Inspection of Table 4 shows that the convergence of ΔE_{HL}^{el} with respect to the basis set is faster at the HF level than at the CCSD and CCSD(T) levels. This reflects the fact that the HF energy converges faster with respect to the one-particle basis set than the correlation energy. The differences in the rates of convergence of the different methods with respect to the basis set are illustrated in Figure 1, in the case where the sequence of basis sets $\{S_{2,n}^{NR}\}_{n=T,Q,5}$ has been used, by the plots for each method $\mathcal{M}$ of the ratios of the calculated energy differences $\Delta E_{HL}^{el}|_{\mathcal{M}/S_{2,n}^{NR}}$ to their CBS values $\Delta E_{HL}^{el}|_{\mathcal{M}/S_{2,\infty}^{NR}}$ ($\mathcal{M}$ = HF, CC, CCSD(T)). Figure 1 shows that, for both complexes, the HF results are already nearly converged when using the smallest basis set (n = T), while the CCSD and CCSD(T) values increase comparatively slowly toward their CBS values. Actually, the convergence of the CC results with respect to the basis set is faster for the Co(II) complex than for the Fe(II) complex (Table 4 and Figure 1). Given that the decrease in the number of paired electrons entailed by the LS → HS change of states is smaller for $[Co(NCH)_6]^{2+}$ than for $[Fe(NCH)_6]^{2+}$ (2 vs 4), this difference in the convergence behaviors can be attributed to the smaller HS−LS differential correlation energy in $[Co(NCH)_6]^{2+}$ than in $[Fe(NCH)_6]^{2+}$.

The use of the two sequences of basis sets $S_{1,n}^{NR}$ (n = T, Q) and $S_{2,n}^{NR}$ (n = T, Q, 5) leads to different CBS values of ΔE_{HL}^{el}, the $S_{1,\infty}^{NR}$ CBS values being systematically more negative than their $S_{2,\infty}^{NR}$ counterparts (Table 4). The $S_{1,T}^{NR}$ and $S_{2,T}^{NR}$ basis sets are identical. The $S_{1,Q}^{NR}$ basis set is far larger than the $S_{2,Q}^{NR}$ basis set (839 vs 539 basis functions). Still, the ΔE_{HL}^{el} values obtained with the $S_{1,Q}^{NR}$ and $S_{2,Q}^{NR}$ basis sets are remarkably close to each other, especially at the CCSD(T) level, at which the values obtained with the two basis sets only differ by 115 cm^{-1} and 38 cm^{-1} for $[Fe(NCH)_6]^{2+}$ and $[Co(NCH)_6]^{2+}$, respectively. Thus, the use of the basis set $S_{2,Q}^{NR}$ in place of the basis set $S_{1,Q}^{NR}$ translates into a huge savings in terms of computational resources with nearly no loss in accuracy. In the series $\{S_{1,n}^{NR}\}_{n=T,Q}$, n is the cardinal number of the basis sets used for the C, N, and TM atoms, whereas in the $\{S_{2,n}^{NR}\}_{n=T,Q,5}$ series it is only the cardinal number of the basis sets used for the TMs, while the N and C atoms remain described by a cc-pVTZ basis set (Table 2). Consequently, the improvement observed for the CC results on going from the n = T to the n = Q basis set in the $\{S_{1,n}^{NR}\}_{n=T,Q}$ sequence of basis sets is primarily due to the enhancement of the quality of the basis set used for the TMs.[39] For this reason, the CBS values of ΔE_{HL}^{el} obtained at the CCSD or CCSD(T) level with the sequence of basis sets $\{S_{2,n}^{NR}\}_{n=T,Q,5}$ are more accurate than those similarly obtained with the $\{\{S_{1,n}^{NR}\}_{n=T,Q}\}$ sequence. For both $[Fe(NCH)_6]^{2+}$ and $[Co(NCH)_6]^{2+}$, the extrapolated $\mathcal{M}/S_{1,\infty}^{NR}$ values of ΔE_{HL}^{el} ($\mathcal{M}$ = CCSD, CCSD(T)) turn out to be better estimates of the $\mathcal{M}/S_{2,5}^{NR}$ values than of the $\mathcal{M}/S_{2,\infty}^{NR}$ values (Table 4).

For both complexes, the ΔE_{HL}^{el} values obtained with the $S_{1,Q}^{NR}$ basis set are systematically slightly more negative than those obtained with the $S_{2,Q}^{NR}$ basis set (Table 4). The two basis sets differ by the basis set put on the C and N atoms of the ligands: cc-pVTZ in $S_{2,Q}^{NR}$ and cc-pVQZ in $S_{1,Q}^{NR}$. Thus, the replacement of the cc-pVQZ basis set put on the ligands by the smaller but still quite flexible cc-pVTZ basis set leads to a slight overestimation

dx.doi.org/10.1021/ct300592w | J. Chem. Theory Comput. 2012, 8, 4216−4231

of the stability of the LS state with regard to the HS state. Given that the metal−ligand bonds are longer in the HS state than in the LS state, this suggests that the loss in accuracy in the description of the metal−ligand bonding entailed by the cc-pVQZ → cc-pVTZ change of basis sets is slightly more pronounced in the HS state than in the LS state.

The expansion of the basis sets in the $\{S^{NR}_{2,n}\}_{n=T,Q,5}$ sequence concerns the TMs only, the C and N atoms of the ligands remaining described by the cc-pVTZ basis set. From the above comparative analysis of the results obtained with the $S^{NR}_{1,Q}$ and $S^{NR}_{2,Q}$ basis sets it follows that for both complexes, the restraint put on the basis sets used for the ligands leads to an overestimation of ΔE^{el}_{HL} in the $S^{NR}_{2,\infty}$ CBS limit. For any of the methods $\mathcal{M}$ used ($\mathcal{M}$ = HF, CCSD, CCSD(T)), a reliable estimate of this overestimation of ΔE^{el}_{HL} is given by the difference $\Delta^{CBS,lig}(\Delta E^{el}_{HL})_{\mathcal{M}}$ between the $S^{NR}_{2,\infty}$ (TQ) and $S^{NR}_{1,\infty}$ CBS values of ΔE^{el}_{HL}, the notation $S^{NR}_{2,\infty}$ (TQ) being used to designate the CBS value extrapolated from the results of the calculations with the $\{S^{NR}_{2,n}\}_{n=T,Q}$ basis sets (Table 4). This difference remains quite small and actually decreases with the level of treatment of the electronic correlation. Thus, at the CCSD(T) level, it amounts to 198 cm^{-1} and 66 cm^{-1} for $[Fe(NCH)_6]^{2+}$ and $[Co(NCH)_6]^{2+}$, respectively. The larger overestimation of ΔE^{el}_{HL} found for $[Fe(NCH)_6]^{2+}$ than for $[Co(NCH)_6]^{2+}$ can be ascribed to the fact that the lengthening of the metal−ligand bond induced by the LS → HS change of states is larger for $[Fe(NCH)_6]^{2+}$ than for $[Co(NCH)_6]^{2+}$.

More generally, the restraint put on the description of the ligands in the sequence of basis sets $\{S^{NR}_{2,n}\}_{n=T,Q,5}$ will systematically lead to an error in the $\mathcal{M}/S^{NR}_{2,\infty}$ CBS value of any quantity Q ($\mathcal{M}$ = HF, CCSD, CCSD(T)). As this was done above for ΔE^{el}_{HL}, we propose to use as a good estimate of this error the difference

$$\Delta^{CBS,lig}(Q)_{\mathcal{M}} = Q|_{\mathcal{M}/S^{NR}_{2,\infty}(TQ)} - Q|_{\mathcal{M}/S^{NR}_{1,\infty}} \quad (11)$$

Our best possible estimate of the CBS value of Q with the method $\mathcal{M}$ is then given by the relation

$$Q|_{\mathcal{M}/CBS(\infty)} = Q|_{\mathcal{M}/S^{NR}_{2,\infty}} - \Delta^{CBS,lig}(Q)_{\mathcal{M}} \quad (12)$$

The most accurate NR estimates of ΔE^{el}_{HL} thus obtained at the CCSD(T)/CBS(∞) level for the complexes $[Fe(NCH)_6]^{2+}$ and $[Co(NCH)_6]^{2+}$ are −2036 cm^{-1} and −3805 cm^{-1}, respectively. They are summarized in Table 6, wherein we also report the ΔE^{el}_{HL} values determined at the HF/CBS(∞) and CCSD/CBS(∞) levels, for they provide us with additional landmarks in the course of our assessment of the other methods.

Height Δ_{JT} of the Barrier to Pseudorotation in the JT-Unstable LS State of $[Co(NCH)_6]^{2+}$. The HF, CCSD, and CCSD(T) values of Δ_{JT} determined using the sequences of basis sets $\{S^{NR}_{1,n}\}_{n=T,Q}$ and $\{S^{NR}_{2,n}\}_{n=T,Q,5}$ and are given in Table 5, along with the corresponding CBS values. All calculated values are positive as expected, and for any of the basis sets used and in the CBS limits, they increase with the level of treatment of electronic correlation as follows:

$$0 < \Delta_{JT}|_{HF} < \Delta_{JT}|_{CCSD} \sim 0.9 \times \Delta_{JT}|_{CCSD(T)} \quad (13)$$

Thus, the height of the barrier is underestimated at the HF level and increases upon the inclusion of correlation effects at the CC level. The CCSD and CCSD(T) values of Δ_{JT} are very close, differing by 25 cm^{-1} at most for the results obtained with the smallest basis set $S^{NR}_{1,T} = S^{NR}_{2,T}$. The convergence of Δ_{JT} with the degree of the CC treatment of electronic correlation is relatively fast, especially when compared to the one previously observed for the HS−LS energy difference. This fast convergence can be ascribed to the fact that the Δ_{JT} energy difference is evaluated for states belonging to the same spin manifold and originating from the same $t_{2g}^6 e_g^1$ ligand-field configuration.

Table 5. Jahn-Teller Instability of the LS State of $[Co(NCH)_6]^{2+}$: NR and DKH Results Obtained at the HF, CCSD, and CCSD(T) Levels for the Height Δ_{JT} (cm^{-1}) of the Barrier to Pseudorotation

	HF	CCSD	CCSD(T)
NR results, $S^{NR}_{1,n}$ (n = T, Q) basis sets			
$S^{NR}_{1,T}$	74	264	289
$S^{NR}_{1,Q}$	88	260	278
$S^{NR}_{1,\infty}$ [a]	99	257	269
NR results, $S^{NR}_{2,n}$ (n = T, Q, 5) basis sets			
$S^{NR}_{2,T} \equiv S^{NR}_{1,T}$	74	264	289
$S^{NR}_{2,Q}$	73	228	251
$S^{NR}_{2,5}$	72	201	220
$S^{NR}_{2,\infty}$ (TQ) [b]	72	202	223
$S^{NR}_{2,\infty}$ [c]	71	185	201
SR shifts $\Delta^{SR}(\Delta_{JT})_{\mathcal{M},n}$ (n = T, Q) as given by eq 6			
n = T	106	101	100
n = Q	106	98	97
$n = \infty$ [d]	106	96	95

[a] CBS values obtained with the $S^{NR}_{1,n}$ (n = T, Q) results and eq 4. [b] CBS values obtained with the $S^{NR}_{2,n}$ (n = T, Q) results and eq 4. [c] CBS values obtained with the $S^{NR}_{2,n}$ (n = T, Q, 5) results and eq 5. [d] CBS values obtained with the n = T and n = Q results and eq 4.

Inspection of Table 5 shows that, at the HF, CCSD, or CCSD(T) level, the convergence of Δ_{JT} with respect to the basis set is also quite fast. The values obtained with the $\{S^{NR}_{1,n}\}_{n=T,Q}$ basis sets are larger than those obtained with the $\{S^{NR}_{2,n}\}_{n=T,Q,5}$ basis sets and, as a consequence thereof, the $S^{NR}_{1,\infty}$ CBS values are also larger than the corresponding $S^{NR}_{2,\infty}$ CBS values. The comparison of the CC results obtained with the $S^{NR}_{1,Q}$ and the smaller $S^{NR}_{2,Q}$ basis set shows that the enhancement of the quality of the basis set used for the Co atom is the main factor responsible for the improvement observed for the CC results on going from the n = T to the n = Q basis set in the $\{S^{NR}_{1,n}\}_{n=T,Q}$ sequence of basis sets. In this respect, the CBS $S^{NR}_{2,\infty}$ values of Δ_{JT} are more accurate than their $S^{NR}_{1,\infty}$ analogues. However, with a given method $\mathcal{M}$ ($\mathcal{M}$ = HF, CCSD, CCSD(T)), and as discussed previously for the determination of ΔE^{el}_{HL}, the restraint put on the description of the ligands in the sequence of basis sets $\{S^{NR}_{2,n}\}_{n=T,Q,5}$ leads to an error in the $\mathcal{M}/S^{NR}_{2,\infty}$ CBS value of Δ_{JT}. For the determination of the estimate $\Delta^{CBS,lig}(\Delta_{JT})_{\mathcal{M}}$ of this error given by eq 11, we have calculated the $\mathcal{M}/S^{NR}_{2,\infty}$(TQ) CBS values of Δ_{JT} (Table 5). By making use of eq 12, we have been able to determine the NR $\mathcal{M}$/CBS(∞) values of Δ_{JT} (Table 6). The most accurate NR estimate of Δ_{JT} thus obtained at the CCSD(T)/CBS(∞) level is 273 cm^{-1}.

3.1.3. Influence of Scalar Relativistic Effects on ΔE^{el}_{HL} and Δ_{JT}. The influence of SR effects on the energy differences ΔE^{el}_{HL} and Δ_{JT} has been evaluated at the HF, CCSD, and CCSD(T) levels according to eq 6, that is, from the results of NR and DKH calculations performed with the NR $\{S^{NR}_{2,n}\}_{n=T,Q}$ and DKH

Table 6. Best NR and DKH CBS Results Obtained at the HF, CCSD, and CCSD(T) Levels for the HS−LS Energy Difference ΔE_{HL}^{el} (cm^{-1}) in $[Fe(NCH)_6]^{2+}$ and $[Co(NCH)_6]^{2+}$, and for Δ_{JT} (cm^{-1}) the Height of the Barrier to Pseudorotation in the Jahn-Teller Unstable LS State of $[Co(NCH)_6]^{2+}$

	$[Fe(NCH)_6]^{2+}$	$[Co(NCH)_6]^{2+}$	
	ΔE_{HL}^{el}	Δ_{JT}	ΔE_{HL}^{el}
nonrelativistic results			
HF/CBS(∞)	−32903	98	−18931
CCSD/CBS(∞)	−6867	240	−5999
CCSD(T)/CBS(∞)	**−2036**	**273**	**−3805**
scalar relativistic DKH results			
HF/CBS(∞)	−31567	204	−18173
CCSD/CBS(∞)	−5531	336	−5307
CCSD(T)/CBS(∞)	**−712**	**368**	**−3111**

$\{S_{2,n}^{NR}\}_{n=T,Q}$ basis sets, respectively. The SR shifts $\Delta^{SR}(\Delta E_{HL}^{el})_{\mathcal{M},n}$ and $\Delta^{SR}(\Delta_{JT})_{\mathcal{M},n}$($\mathcal{M}$ = HF, CCSD, CCSD(T)) obtained with the different basis sets (n = T, Q) as well as their extrapolated CBS values (n = ∞) are given in Tables 4 and 5, respectively. All these values are positive: SR effects increase the HS−LS energy difference in $[Fe(NCH)_6]^{2+}$ and in $[Co(NCH)_6]^{2+}$, and also the height Δ_{JT} of the barrier to pseudorotation in the LS state of $[Co(NCH)_6]^{2+}$. Further inspection of Tables 4 and 5 shows that the predicted SR shifts are only marginally affected by the degree of treatment of electron correlation and that they have a weak dependence on the quality of the basis sets used. The CCSD and CCSD(T) values are indeed very close and depart very little from the HF values. As for the influence of the quality of the basis sets, it is vanishing at the HF level while the CC values of the SR shifts turn out to be nearly converged for the smallest basis sets (n = T). Similar observations were made by Balabanov and Peterson regarding the weak influence of both the electron correlation treatment and the size of the basis set on the SR shifts to the energies of the $4s^23d^{m-2} \rightarrow 4s^13d^{m-1}$ excitations in the Sc−Cu series of TMs.[106]

The most accurate estimates of the SR shifts to the HS−LS energy differences in $[Fe(NCH)_6]^{2+}$ and $[Co(NCH)_6]^{2+}$ are $\Delta^{SR}(\Delta E_{HL}^{el})_{CCSD(T),\infty}$ = 1336 cm^{-1} and $\Delta^{SR}(\Delta E_{HL}^{el})_{CCSD(T),\infty}$ = 694 cm^{-1}, respectively. For the barrier to pseudorotation in LS $[Co(NCH)_6]^{2+}$, the best estimate of the shift is $\Delta^{SR}(\Delta_{JT})_{CCSD(T),\infty}$ = 95 cm^{-1}. Thus, for ΔE_{HL}^{el} and Δ_{JT}, the SR shifts are on the same order of magnitude as their NR-CCSD(T)/CBS(∞) values (Table 6). Relativistic effects should therefore systematically be included in the studies of the energetics of first-row TM complexes. The final DKH-CCSD(T)/CBS(∞) best estimates of ΔE_{HL}^{el} are −712 cm^{-1} and −3111 cm^{-1} for $[Fe(NCH)_6]^{2+}$ and $[Co(NCH)_6]^{2+}$, respectively, and the final DKH-CCSD(T)/CBS(∞) best estimate of Δ_{JT} is 368 cm^{-1}. These values are reported in Table 6 along with those similarly obtained at the DKH-HF and DKH-CCSD levels.

For both complexes, the vibrational contribution ΔE_{HL}^{vib} to the HS−LS zero-point energy difference ΔE_{HL}° are negative because of the weakening of the metal−ligand bonds upon the LS → HS change of spin states (data not shown). Consequently, the DKH-CCSD(T)/CBS(∞) values of ΔE_{HL}^{el} being negative ($\Delta E_{HL}^{\circ} = \Delta E_{HL}^{el} + \Delta E_{HL}^{vib}$), the two complexes are found to be HS species.

3.2. Performance of the CASPT2 Method. Starting from a CASSCF reference wave function, which captures all near-degeneracy effects in the electronic structure of the investigated system, the CASPT2 method is formulated to recover the remaining correlation by adding a second-order perturbative correction to the electronic energy.[43,44] In its initial formulation, the CASPT2 approach was successfully applied to numerous chemical problems, but the original one-electron zeroth-order Hamiltonian was shown to systematically favor open-shell over closed-shell systems.[134,135] Modifications of the one-electron zeroth-order Hamiltonian were devised to remedy the situations. These are the $g1$, $g2$, and $g3$ modifications,[136] which have been superseded by the IPEA shift technique.[45] The latter involves the introduction of a level shift in the zeroth-order Hamiltonian, the so-called ionization potential−electron affinity (IPEA) shift, whose standard value was set to ε = 0.25 au based on test calculations of dissociation energies, spectroscopic constants, excitation, and ionization energies of atoms and molecules.[45] However, from the study of the IPEA dependence of the CASPT2 values of ΔE_{HL}^{el} in $[Fe(NCH)_6]^{2+}$ and in Fe(II) complexes having also a $[FeN_6]$ core and of experimentally known magnetic behaviors, it was suggested that an IPEA shift of 0.50−0.70 au should rather be used for the CASPT2 determination of ΔE_{HL}^{el} in such Fe(II) complexes.[46] Due to the $[FeN_6]$ core found in many Fe(II) SCO complexes, $[Fe(NCH)_6]^{2+}$ has been the subject of several CASPT2 studies.[9,46,137,138] Here, we examine the influence of the IPEA parameter on the CASPT2 HS−LS energy differences in $[Fe(NCH)_6]^{2+}$ and in $[Co(NCH)_6]^{2+}$ on the basis of the CC results.

3.2.1. The HS−LS Energy Difference in $[Fe(NCH)_6]^{2+}$ and in $[Co(NCH)_6]^{2+}$. The DKH CASSCF/CASPT2 calculations have been performed with the ANO-I and ANO-II basis sets, which are slightly modified versions of basis sets used in a recent CASPT2 study of heme models.[47] ANO-RCC basis sets like the ANO-I basis set should help reach convergence in the HS−LS energy differences at an affordable computational cost.[46,137] With the larger ANO-II basis set, in which the TMs are described by the largest possible contraction available for them in the ANO-RCC basis sets of the MOLCAS library, the results should be close to the basis set limit.[47] For both complexes in either spin-state, the CASSCF wave functions are dominated by a single determinant with a weight larger than 90%, and the natural orbital occupation numbers for the active space are near two and zero and near one for open-shell states (see Supporting Information), thus reflecting as anticipated above the low multireference character of the considered electronic states.[127,139] The CASSCF values of the HS−LS energy differences are summarized in Table 7. They have a weak dependence on the basis set and are intermediate between the DKH-HF/CBS(∞) and the DKH-CCSD/CBS(∞) results (Table 6).

The dependencies on the IPEA shift ε of the CASPT2 ΔE_{HL}^{el} values in the $[M(NCH)_6]^{2+}$ complexes (M = Fe, Co) are plotted in Figure 2. For the considered ε values, passing from the ANO-I to the ANO-II basis set translates into a systematic increase of ΔE_{HL}^{el} of ∼800 cm^{-1} and ∼500 cm^{-1} for $[Fe(NCH)_6]^{2+}$ and $[Co(NCH)_6]^{2+}$, respectively. At ε = 0, the DKH-CCSD(T)/CBS(∞) best estimates of −712 cm^{-1} and −3111 cm^{-1} found for $[Fe(NCH)_6]^{2+}$ and $[Co(NCH)_6]^{2+}$, respectively, are severely underestimated, as expected. The results improve with increasing ε values. For $[Fe(NCH)_6]^{2+}$, although the geometries, the active space, and the basis sets

Table 7. CASSCF Results for the HS−LS Energy Difference ΔE_{HL}^{el} (cm^{-1}) in $[Fe(NCH)_6]^{2+}$ and $[Co(NCH)_6]^{2+}$, and for the Height Δ_{JT} (cm^{-1}) of the Barrier to Pseudorotation and the Jahn-Teller Stabilization Energy E_{JT} (cm^{-1}) in the Jahn-Teller Unstable LS State of $[Co(NCH)_6]^{2+}$: Results of Scalar Relativistic Calculations Performed with the ANO-I and ANO-II Basis Sets

	$[Fe(NCH)_6]^{2+}$	$[Co(NCH)_6]^{2+}$		
	ΔE_{HL}^{el}	ΔE_{HL}^{el}	Δ_{JT}	E_{JT}
ANO-I	−18257	−12360	491	1908
ANO-II	−17959	−12188	541	1972

used differ, the IPEA dependency of ΔE_{HL}^{el} compares well with the one reported in ref 46. For this complex, the DKH-CCSD(T)/CBS(∞) best estimate of ΔE_{HL}^{el} is obtained at $\varepsilon \approx 0.60$ au and at $\varepsilon \approx 0.45$ au, when using the ANO-I and ANO-II basis sets, respectively. This supports the recommended use of an IPEA value of 0.50−0.70 au for the CASPT2 studies of the spin-state energetics in $[Fe(NCH)_6]^{2+}$ and in Fe(II) complexes with a $[FeN_6]$ core.[46]

For $[Co(NCH)_6]^{2+}$, the DKH-CCSD(T)/CBS(∞) best estimate of ΔE_{HL}^{el} is obtained for larger IPEA values: at $\varepsilon \approx 1.25$ au and $\varepsilon \approx 1.05$ au, when using the ANO-I and ANO-II basis sets, respectively. This suggests that, using basis sets similar to the ANO-I and ANO-II basis sets, a IPEA value of 1.00−1.30 au is best suited for the CASPT2 characterization of the spin-state energetics in Co(II) complexes with a $[CoN_6]$ core.

3.2.2. The Jahn−Teller Instability of the LS State of $[Co(NCH)_6]^{2+}$. For $[Co(NCH)_6]^{2+}$ in the JT unstable LS state, the CASSCF values obtained with the ANO-I and ANO-II basis sets for the height Δ_{JT} of the barrier to pseudorotation and for the JT stabilization energy E_{JT} are given in Table 7. They are positive, as expected, and vary little with the basis set. The CASSCF Δ_{JT} values are actually much larger than the DKH HF and CC best estimates (Table 6). The influence of the IPEA shift on the CASPT2 determination of Δ_{JT} and E_{JT} has been probed. The results are summarized in Figure 3.

For the considered IPEA values, passing from the ANO-I to the ANO-II basis set translates into a systematic small increase of the CASPT2 values of Δ_{JT} and E_{JT} of about 70 cm^1 and 80 cm^{-1}, respectively. The CASPT2 estimates of Δ_{JT} and E_{JT} are both slowly increasing functions of the IPEA shift ε. This contrasts with the strong IPEA dependencies observed for the CASPT2 values of ΔE_{HL}^{el} in $[Co(NCH)_6]^{2+}$ and in $[Fe(NCH)_6]^{2+}$ (Figure 2) and which are due to the large modification of the electronic structures entailed by the change of spin states.[45] The CASPT2 values of Δ_{JT} at $\varepsilon = 0$ are too small compared to the DKH-CCSD(T)/CBS(∞) best estimate of 368 cm^{-1}, which is obtained at $\varepsilon \approx 2.15$ au and $\varepsilon \approx 1.50$ au, when using the ANO-I and the ANO-II basis sets, respectively. These optimal IPEA values are larger than those found for the CASPT2 calculations of ΔE_{HL}^{el} in $[Co(NCH)_6]^{2+}$. Still, using the IPEA value of 1.00−1.30 au which seems best suited for the CASPT2 characterization of the spin-state energetics in the complex, reasonably good CASPT2 estimates of Δ_{JT} are obtained with the two basis sets. From the CASPT2 results obtained with this IPEA value of 1.00−1.30 au, a best *ab initio* estimate of 1600 ± 100 cm^{-1} is obtained for E_{JT}

3.3. Performances of DFT Methods. The search for accurate density functional approximations is a very active research area. Numerous functionals are regularly designed either nonempirically so as to satisfy as many exact theoretical constraints as possible or by empirical fitting to accurate experimental or *ab initio* data. A comprehensive view of the many kinds of functionals is beyond the scope of the present study. Our objective here is to assess the performance of popular XC energy functionals for the accurate determination of the HS−LS energy difference in $[Fe(NCH)_6]^{2+}$ and in $[Co(NCH)_6]^{2+}$, and for that of the height Δ_{JT} of the barrier to pseudorotation in LS $[Co(NCH)_6]^{2+}$. These functionals can be classified as semilocal, hybrid, range-separated hybrid, and double-hybrid density functionals. To make these distinctions clear, we give below a brief overview of the different types of considered density functionals. The reader is referred to the referenced papers for more details.

Local and semilocal XC energy functionals admit the general form

$$E_{xc}[\rho_\uparrow, \rho_\downarrow] = \int d\mathbf{r}\, \rho(\mathbf{r}) \varepsilon_{xc}(\rho_\uparrow(\mathbf{r}), \rho_\downarrow(\mathbf{r}), \nabla\rho_\uparrow(\mathbf{r}), \nabla\rho_\downarrow(\mathbf{r}), \nabla^2\rho_\uparrow(\mathbf{r}), \nabla^2\rho_\downarrow(\mathbf{r}), \tau_\uparrow(\mathbf{r}), \tau_\downarrow(\mathbf{r})) \quad (14)$$

where $\rho_\uparrow(\mathbf{r})$ and $\rho_\downarrow(\mathbf{r})$ are the spin-up and spin-down densities, $\rho(\mathbf{r}) = \rho_\uparrow(\mathbf{r}) + \rho_\downarrow(\mathbf{r})$ is the charge density, and ε_{xc} is the XC energy *per* particle. In the local density approximation (LDA) not considered here, ε_{xc} depends only on the spin

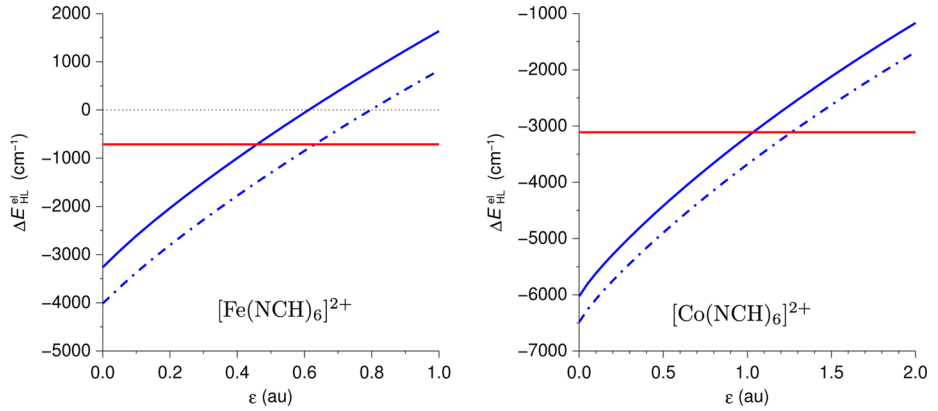

Figure 2. Dependence of the CASPT2 HS−LS energy differences in $[Fe(NCH)_6]^{2+}$ and $[Co(NCH)_6]^{2+}$ on the IPEA shift ε: CASPT2 results obtained with the ANO-I (blue dot-dashed lines) and ANO-II (blue solid lines) basis sets. The DKH-CCSD(T)/CBS(∞) best estimates are also shown (horizontal red lines).

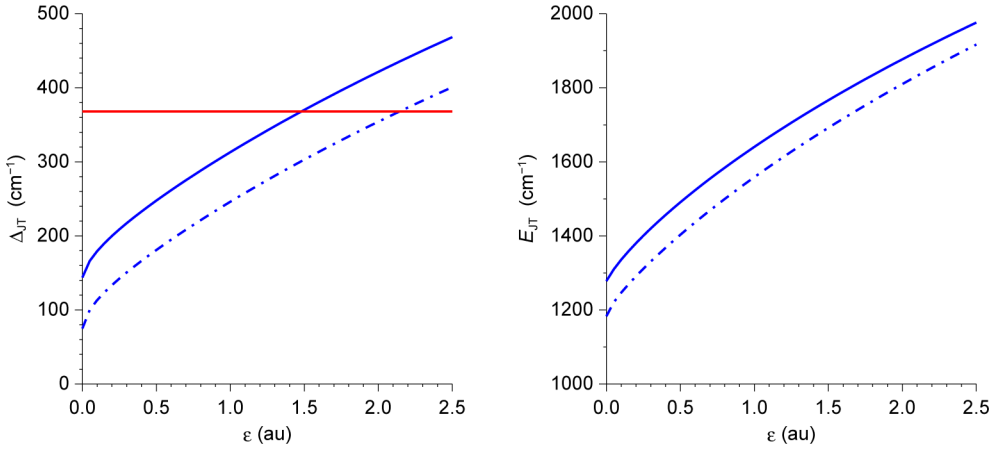

Figure 3. CASPT2 characterization of $[Co(NCH)_6]^{2+}$ in the Jahn−Teller unstable LS state: plots of the CASPT2/ANO-I (blue dot-dashed lines) and CASPT2/ANO-II (blue solid lines) values of Δ_{JT} and E_{JT} as functions of the IPEA shift ε; the solid red line (left) represents the DKH-CCSD(T)/CBS(∞) best estimate of Δ_{JT}.

densities.[8,140−145] Although the LDA is only valid for slowly varying densities, it performs reasonably for the description of atomic, molecular, and solid systems. For these systems characterized by rapidly varying densities, the LDA underestimates the exchange energy by about 14% and overestimates the correlation energy by a factor of approximately 2.5; quite often the two errors cancel.[146,147] Semilocal approximations improve on the LDA by including corrections which reflect the strongly inhomogeneous densities of real systems. Within the generalized gradient approximation (GGA), ε_{xc} depends on the spin densities but also on their gradients $\nabla\rho_\sigma(\mathbf{r})$ ($\sigma = \uparrow,\downarrow$).[62,64,148−150] In the meta-GGA,[79,80,151,152] ε_{xc} is also a function of the second derivatives of the spin densities $\nabla^2\rho_\sigma(\mathbf{r})$ and/or the kinetic energy densities $\tau_\sigma(\mathbf{r})$.

$$\tau_\sigma(\mathbf{r}) = \frac{1}{2}\sum_{i\sigma}^{\text{occ.}} f_{i\sigma}\,|\nabla\psi_{i\sigma}(\mathbf{r})|^2 \tag{15}$$

where $f_{i\sigma}$ and $\psi_{i\sigma}(\mathbf{r})$ are the occupation number and the spin−orbital of the ith σ-type single-particle level of the Kohn−Sham (KS) noninteracting system, and the summation runs over the occupied spin−orbitals.

With their conceptual root in the adiabatic connection formalism,[153−158] hybrid XC energy functionals include a contribution of the nonlocal HF exchange energy:[60,159]

$$E_x^{HF}[\rho_\uparrow,\rho_\downarrow] = -\frac{1}{2}\sum_{\sigma=\uparrow,\downarrow}\sum_{i,j}^{\text{occ}}\iint d\mathbf{r}_1\, d\mathbf{r}_2\, \psi_{i\sigma}^*(\mathbf{r}_1)\psi_{j\sigma}^*(\mathbf{r}_1)\frac{1}{r_{12}}\psi_{i\sigma}(\mathbf{r}_2)\psi_{j\sigma}(\mathbf{r}_2) \tag{16}$$

They explicitly depend on the occupied KS spin−orbitals ($E_x^{HF}[\rho_\uparrow,\rho_\downarrow] \equiv E_x^{HF}[\{\psi_{i\sigma}\}_{i\sigma\in\text{occ}}]$) and can be written

$$E_{xc}^{hyb}[\rho_\uparrow,\rho_\downarrow] = a_x E_x^{HF}[\rho_\uparrow,\rho_\downarrow] + (1-a_x)E_x^{sem}[\rho_\uparrow,\rho_\downarrow] + E_c^{sem}[\rho_\uparrow,\rho_\downarrow] \tag{17}$$

where $a_x \in]0,1]$, and E_x^{sem} and E_c^{sem} are semilocal exchange and correlation functionals. With their fixed amounts of HF exchange, these functionals are also termed global hybrids to distinguish them from the other types of hybrid functionals.

The considered range-separated hybrid (RSH) functionals rely on the splitting of the Coulomb operator into a short-range (sr) and a long-range (lr) term according to:[86,89−91,160−163]

$$\frac{1}{r_{12}} = \underbrace{\frac{1-[\alpha+\beta\,\text{erf}(\omega r_{12})]}{r_{12}}}_{v_{ee}^{sr}(r_{12})} + \underbrace{\frac{\alpha+\beta\,\text{erf}(\omega r_{12})}{r_{12}}}_{v_{ee}^{lr}(r_{12})}, \tag{18}$$

where "erf" is the error function and ω, the range separation parameter. The short-range component dominates for small interelectronic distances, $r_{12} \ll 1/\omega$, and behaves like $(1-\alpha)/r_{12}$ for $r_{12} \to 0$. The long-range component dominates for $r_{12} \gg 1/\omega$, with an asymptotic behavior in $(\alpha+\beta)/r_{12}$. One thus must verify $(\alpha,\beta) \in [0,1]^2$ and $0 \le \alpha + \beta \le 1$. The splitting of the Coulomb operator allows for a partition of the exchange energy into a short-range and a long-range component:

$$E_x[\rho_\uparrow,\rho_\downarrow] = E_x^{sr}[\rho_\uparrow,\rho_\downarrow] + E_x^{lr}[\rho_\uparrow,\rho_\downarrow] \tag{19}$$

The short-range component E_x^{sr} is approximated by a local or semilocal functional, and the long-range complement is described by the HF exchange

$$E_x^{lr}[\rho_\uparrow,\rho_\downarrow] = -\frac{1}{2}\sum_{\sigma=\uparrow,\downarrow}\sum_{i,j}^{\text{occ}}\iint d\mathbf{r}_1\, d\mathbf{r}_2\, \psi_{i\sigma}^*(\mathbf{r}_1)\psi_{j\sigma}^*(\mathbf{r}_1)v_{ee}^{lr}(r_{12})\psi_{i\sigma}(\mathbf{r}_2)\psi_{j\sigma}(\mathbf{r}_2) \tag{20}$$

There are two approaches to the design of RSH exchange energy functionals based on eq 18. In the LC scheme,[89,90,163] $\alpha = 0$ and $\beta = 1$: the exchange energy functional is the combination of the long-range HF exchange and the chosen short-range semilocal exchange functional; furthermore, the exchange potential has the correct $-1/r_{12}$ asymptotic behavior. In the CAM approach,[86,91] $\alpha \neq 0$, so that there is a nonvanishing amount "α" of HF exchange at short-range, and the correct asymptotic behavior of the exchange potential is retained for $\alpha + \beta = 1$. Finally, a RSH XC energy functional is obtained by combining a RSH exchange energy functional with an unmodified semilocal correlation energy functional.

Inspired by the Görling-Levy perturbation theory,[164,165] the double-hybrid approach substitutes in global hybrid functionals a fraction of the semilocal correlation energy by a nonlocal

second-order Møller−Plesset (MP2) type correlation energy.[87,88,166] Double-hybrid XC energy functionals thus read

$$E_{xc}^{dbl\text{-}hyb}[\rho_\uparrow, \rho_\downarrow] = a_x E_x^{HF}[\rho_\uparrow, \rho_\downarrow] + (1 - a_x)E_x^{sem}[\rho_\uparrow, \rho_\downarrow] + (1 - a_c)E_c^{sem}[\rho_\uparrow, \rho_\downarrow] + a_c E_c^{MP2}[\rho_\uparrow, \rho_\downarrow] \quad (21)$$

where $(a_x,a_c) \in]0,1]^2$ and $E_c^{MP2}[\rho_\uparrow,\rho_\downarrow]$, the nonlocal MP2-like contribution, is given in spin−orbital form by

$$E_c^{MP2}[\rho_\uparrow, \rho_\downarrow] \equiv E_c^{MP2}[\{\psi_i\}_{i\in occ}, \{\psi_a\}_{a\in virt}] = \frac{1}{4} \sum_{\substack{ij\in occ \\ ab\in virt}} \frac{[(ia|jb) - (ib|ja)]^2}{\varepsilon_i + \varepsilon_j - \varepsilon_a - \varepsilon_b} \quad (22)$$

The labels i and j (respectively, a and b) are for the occupied (respectively, virtual) KS spin−orbitals ($\psi_k \equiv \psi_{k\sigma_k}$) of energies ε_k ($k = i,j,a,b$), and $(ia|jb)$ is a two-electron repulsion integral in Mulliken notation. For the evaluation of the double-hybrid correlation energy, the KS spin−orbitals are first self-consistently determined using the hybrid XC energy functional defined by the first three terms of the right-hand side of eq 21, then used for the evaluation of the nonlocal correlation contribution.[87,88,166]

With their explicit dependency on both occupied and virtual KS spin−orbitals, double-hybrid XC energy functionals are at the highest (fifth) rung of John Perdew's Jacob's ladder of density functional approximations,[167] with the LDA, GGA, meta-GGA, and hybrid functionals at the first, second, third, and fourth rungs, respectively. We will now discuss the performances of the selected functionals, which thus span the second to fifth rungs of the ladder. As explained in the Computational Details section, the DFT calculations were run nonrelativistically. Hence, the performances of the functionals will be assessed against the NR-CCSD(T)/CBS(∞) results.

3.3.1. HS−LS Energy Differences in $[Fe(NCH)_6]^{2+}$ and in $[Co(NCH)_6]^{2+}$. The results obtained with the different functionals for the NR values of the HS−LS energy differences in the two complexes are summarized in Table 8. The inspection of this table shows that the functionals perform very differently and that most of them actually are not even in the right ballpark. The NR-CCSD(T)/CBS(∞) estimates of ΔE_{HL}^{el} in $[Fe(NCH)_6]^{2+}$ and $[Co(NCH)_6]^{2+}$ are −2036 cm^{-1} and −3805 cm^{-1}, respectively.

With the exception of the HCTH/407 and HCTH/407+ functionals, the GGAs strongly overestimate ΔE_{HL}^{el} and thus tend to fail to predict the HS state as the electronic ground state of the complexes. Among these GGA results, the less inaccurate ones are those obtained with the functionals including the semiempirical OPTX exchange functional,[71] namely, the OLYP[63,71] and OPBE[58,59,71] GGAs, the former leading to a lesser overestimation of ΔE_{HL}^{el} than the latter. The HCTH/407 functional[74] is a semiempirical XC energy GGA obtained by fitting to a training set containing 407 molecular and atomic systems, with no data relative to the spin-state energetics of TM complexes. It gives for $[Fe(NCH)_6]^{2+}$ the best GGA estimate of ΔE_{HL}^{el}, which it however underestimates by 35.8%, and it overestimates ΔE_{HL}^{el} for $[Co(NCH)_6]^{2+}$. The HCTH/407+ functional is a reparametrization of the HCTH/407 obtained by including the ammonia dimer $(NH_3)_2$ in the training set, with special emphasis on the improved description of the nonlinear hydrogen bond and the potential energy surface of this dimer.[76] In the present case, passing from the HCTH/407 to the HCTH/407 + GGA translates into a decrease of the ΔE_{HL}^{el} values. For $[Fe(NCH)_6]^{2+}$, this accentuates the overestimation of the stability of the HS state with regard to the LS state and leads, for $[Co(NCH)_6]^{2+}$, to a minor improvement.

Table 8. NR DFT Results for the HS−LS Energy Difference ΔE_{HL}^{el} (cm^{-1}) in the $[M(NCH)_6]^{2+}$ Complexes (M = Fe, Co)[a]

GGAs	M = Fe	M = Co	hybrid GGAs	M = Fe	M = Co
PBE	8470	3021	B3LYP	−1726	−2483
BLYP	6282	2145	B3LYP*	441	−1213
BP86	9300	3468	X3LYP	−2145	−2788
BOP	4951	1705	PBE0	−3138	−3579
PBEOP	5394	1830	B97	−2789	−2982
OLYP	118	−495	B97−3	−5989	−4673
OPBE	1706	192	B98	−3067	−3258
HCTCH/407	−2764	−1571	mPW1K	−9190	−7038
HCTCH/407+	−4255	−2195			
meta-GGAs	M = Fe	M = Co	hybrid meta-GGAs	M = Fe	M = Co
TPSS	8432	2481	BB1K	−6411	−5408
PKZB	2884	465	TPSSh	3602	−220
M06-L	545	−1808	M05	−9180	−5369
			M06	−4789	−3467
range-separated hybrids	M = Fe	M = Co	double hybrids	M = Fe	M = Co
CAM-B3LYP	−2002	−2706	B2-PLYP	−1119	−2829
LC-BLYP	6877	2032	mPW2-PLYP	−2585	−3662
LC-PBE	9478	3136			
CAM-PBE0	−672	−2657			

[a]The results were obtained with the $S_{2,Q}^{NR}$ basis set except in the case of the double-hybrid XC energy functionals, for which the reported results correspond to those obtained with the $\{S_{2,n}^{NR}\}_{n=T,Q,5}$ basis sets extrapolated to the CBS limit.

The tested meta-GGA functionals severely overestimate the HS−LS energy differences in the two complexes. The smallest overestimation is observed for the semiempirical M06-L functional, which was obtained by fitting to 22 energetic databases, for main-group thermochemistry, TM bonding, thermochemical kinetics, and noncovalent interactions.[82] The tendency of the GGA and meta-GGA functionals to overestimate ΔE_{HL}^{el} can be ascribed to the fact that they still present the underestimation of exchange inherited from their LDA component.[18,20] The approximate exchange energy functionals must indeed correctly account for the variation of the exchange interaction with increasing or decreasing spin polarization, as in the case of a change of spin states. The performances of the highly parametrized HCTH/407, HCTH/407+, and M06-L functionals trained on large data sets, though far from being satisfactory, suggest that semiempirical semilocal XC functionals for accurate spin-state energetics of TM complexes could be designed by including in such training sets highly accurate data like those reported here for $[Fe(NCH)_6]^{2+}$ and $[Co(NCH)_6]^{2+}$.

Contrary to the trend observed for the semilocal functionals, the assessed global hybrids tend to give the correct sign for ΔE_{HL}^{el}. This is in line with the fact that the inclusion of a contribution of the nonlocal HF exchange generally leads to improvements.[60,68,69,159] The improvement observed here can be ascribed to the fact that the admixture of HF exchange helps

correct for the underestimation of the exchange interaction by the semilocal functionals. There however remains the general question of the optimal amount a_x of HF exchange to use. Global hybrids incorporating a fraction of $a_x \approx 0.20-0.25$ of HF exchange tend to perform well for main group compounds.[60,68,69,159] For the spin-state energetics of TM complexes, the stability of states of high spin multiplicities with regard to those of lower spin multiplicities is known to increase with a_x and to become severely overestimated for too large a_x values.[11,12,20] Despite the different functional forms of the tested global hybrids, the inspection of Table 8 shows that, except for B97 ($a_x \approx 0.194$), this trend holds for the hybrid GGAs (B3LYP*, $a_x = 0.150$; B3LYP, $a_x = 0.200$; X3LYP, $a_x \approx 0.218$; B98, $a_x \approx 0.220$; PBE0, $a_x = 0.250$; B97-3, $a_x \approx 0.269$; mPW1K, $a_x = 0.428$), and to a lesser extent, also for the tested hybrid meta-GGAs (TPSSh, $a_x = 0.100$; M06, $a_x = 0.270$; M05, $a_x = 0.280$; BB1K, $a_x = 0.420$). On the basis of assessments made mostly against experimental data, global hybrids with some 10% of HF exchange (like the B3LYP* and TPSSh) are proposed as the ones best suited for the description of the properties of the TM complexes, their spin-state energetics included.[11,12,15,18,20,34,37,168] Here, the B3LYP* and TPSSh functionals strongly overestimate the HS−LS energy difference in both complexes. For either complex, results intermediate between the NR-CCSD and NR-CCSD(T) best estimates (Table 6) are observed for global hybrids with $a_x \approx 0.2-0.3$. Actually, the X3LYP ($a_x \approx 0.218$) and PBE0 ($a_x = 0.250$) functionals perform remarkably well for $[Fe(NCH)_6]^{2+}$ and $[Co(NCH)_6]^{2+}$, respectively, their predicted ΔE_{HL}^{el} values differing from the NR-CCSD(T)/CBS(∞) estimates only by −5.4% and +5.9%, respectively. It thus follows that the question of the optimal amount of HF exchange to include in global hybrids for TM spin-state energetics remains open.

The use of the four RSHs did not lead to a systematic improvement of the DFT results. The CAM-B3LYP functional ($\alpha = 0.19$, $\beta = 0.46$, $\omega = 0.33$ bohr^{-1})[86] gives for $[Fe(NCH)_6]^{2+}$ a ΔE_{HL}^{el} value in exceptionally good agreement with the NR *ab initio* best estimate (+1.7%), but for $[Co(NCH)_6]^{2+}$, it overestimates ΔE_{HL}^{el} by 28.9%. The LC-BLYP ($\alpha = 0$, $\beta = 1$, $\omega = 0.33$ bohr^{-1}) and LC-PBE ($\alpha = 0$, $\beta = 1$, $\omega = 0.30$ bohr^{-1}) functionals[89,90] severely overestimate ΔE_{HL}^{el} for the two complexes. The CAM-PBE0 functional ($\alpha = 0.25$, $\beta = 0.75$, $\omega = 0.30$ bohr^{-1})[91] predicts for $[Fe(NCH)_6]^{2+}$ and $[Co(NCH)_6]^{2+}$ the correct sign of ΔE_{HL}^{el}, like the CAM-B3LYP, but it overestimates ΔE_{HL}^{el} in both cases, by 67.0% and 30.2%, respectively. Interestingly however, ones notes for these RSHs characterized by $\omega \approx 0.3$ bohr^{-1} that the LC-PBE and LC-BLYP actually perform like the PBE and BLYP GGAs, and that the CAM-PBE0 and CAM-B3LYP functionals characterized by $\alpha \neq 0$ give the most acceptable results. This indicates the need of a nonvanishing amount of HF exchange at short-range, which is in line with the fact that the electronic rearrangement accompanying the LS ↔ HS change of states is centered on the TMs and mainly takes place in the compact 3d shell of TMs. Increasing ω and/or modifying α therefore constitute a convenient and attractive means to readily tune the performance of RSHs for TM spin-state energetics.

The tested double-hybrid B2-PLYP ($a_x = 0.53$, $a_c = 0.27$) and mPW2-PLYP ($a_x = 0.55$, $a_c = 0.25$)[87,88] functionals predict for the two complexes the correct sign for ΔE_{HL}^{el}. The B2-PLYP functional overestimates the ΔE_{HL}^{el} values. The mPW2-PLYP functional performs very well for $[Co(NCH)_6]^{2+}$ (+3.8%), but for $[Fe(NCH)_6]^{2+}$, it underestimates ΔE_{HL}^{el} (−27.0%). The two double hybrids have the same LYP correlation functional[63] and similar a_x and a_c optimized values, so that the observed better performance of the mPW2-PLYP with regard to the B2-PLYP can be ascribed to the replacement of the B exchange functional[62] by the mPW exchange functional.[169] Remarkably, the mPW2-PLYP functional proves to be the only tested functional to give ΔE_{HL}^{el} values that are within ±2 kcal/mol (*ca.* ± 700 cm^{-1}) of the best *ab initio* estimates. No functional gives for both complexes ΔE_{HL}^{el} values which are within chemical accuracy (±1 kcal/mol) of the best *ab initio* estimates.

3.3.2. Height Δ_{JT} of the Barrier to Pseudorotation in the JT-Unstable LS State of $[Co(NCH)_6]^{2+}$. The NR-CCSD(T)/CBS(∞) value of the barrier height Δ_{JT} is 273 cm^{-1}. The Δ_{JT} values obtained with the different density functionals are given in Table 9. Although the predicted DFT values are all positive as expected, the inspection of this table shows that Δ_{JT} is overestimated by most functionals by a factor of ∼1.4 at least. The use of the M06-L and CAM-PBE0 functionals leads to a 30−40% underestimation of Δ_{JT}. The LC-BLYP value is in reasonable agreement with the best *ab initio* estimate. An almost perfect match is observed for the LC-PBE functional and also for the semiempirical mPW1K and BB1K functionals, which were actually devised for main-group thermochemical kinetics.[75,78] Although the functionals mPW1K and BB1K perform badly for the HS−LS energy difference in $[M(NCH)_6]^{2+}$ (M = Fe, Co), their remarkable performances for the determination of Δ_{JT} suggest that they may be well suited for the study of the reactions of first-row TM complexes in a given spin state.

Table 9. NR DFT Results for the Height Δ_{JT} (cm^{-1}) of the Barrier to Pseudorotation in the Jahn-Teller Unstable LS State of $[Co(NCH)_6]^{2+}$[a]

GGAs		hybrid GGAs	
PBE	590	B3LYP	511
BLYP	664	B3LYP*	595
BP86	592	X3LYP	473
BOP	775	PBE0	428
PBEOP	727	B97	577
OLYP	962	B97−3	571
OPBE	954	B98	516
HCTCH/407	994	mPW1K	256
HCTCH/407 +	1066		
meta-GGAs		**hybrid meta-GGAs**	
TPSS	498	BB1K	284
PKZB	761	TPSSh	457
M06-L	185	M05	558
		M06	390
range-separated hybrid		**double hybrids**	
CAM-B3LYP	375	B2-PLYP	488
LC-BLYP	312	mPW2-PLYP	415
LC-PBE	280		
CAM-PBE0	153		

[a]The results were obtained with the $S_{2,Q}^{NR}$ basis set except in the case of the double-hybrid XC energy functionals, for which the reported results correspond to those obtained with the $\{S_{2,n}^{NR}\}_{n=T,Q,5}$ basis sets extrapolated to the CBS limit.

4. SUMMARY, CONCLUSION, AND OUTLOOK

Highly accurate estimates of the HS−LS energy difference ΔE_{HL}^{el} in the HS complexes $[Fe(NCH)_6]^{2+}$ and $[Co(NCH)_6]^{2+}$

and of the height Δ_{JT} to pseudorotation in LS $[Co(NCH)_6]^{2+}$ have been obtained from the results of intensive CCSD(T) calculations extrapolated to the CBS limits. SR effects were taken into account and shown to significantly influence the energetics of the complexes. The SR shifts, which proved to have been accurately determined already at the HF level, are indeed on the same order of magnitude as the NR values of ΔE^{el}_{HL} and Δ_{JT}. The influence of relativistic effects should therefore systematically be probed, especially when computational results have to be compared against experimental data. Actually, given that the spin-state energetics of TM complexes can be strongly influenced by their surroundings and also by temperature and pressure, the calibration of computational methods against experimental data should be avoided unless special care is taken to accurately account for the influence of these external factors. For this purpose, it is preferable to use highly accurate gas-phase *ab initio* data like those reported here for $[Fe(NCH)_6]^{2+}$ and $[Co(NCH)_6]^{2+}$

We have used the CCSDT/CBS(∞) estimates of the energy differences ΔE^{el}_{HL} and Δ_{JT} to assess the performances of the CASPT2 method and of 30 functionals of the GGA, meta-GGA, global hybrid, RSH, and double-hybrid types. For the CASPT2 method, our results confirm that an IPEA parameter value of 0.50−0.70 au seems best suited for the study of the spin-state energetics of Fe(II) complexes with a $[FeN_6]$ core.[46,138] They also indicate that this parameter should be increased to 1.00−1.30 au when dealing with the spin-state energetics of Co(II) complexes with a $[CoN_6]$ core. For $[Co(NCH)_6]^{2+}$ in the JT unstable LS state, with the IPEA value of 1.00−1.30 au, accurate results are obtained for the height Δ_{JT} of the barrier to pseudorotation, and a JT stabilization energy of E_{JT} = 1600 ± 100 cm^{-1} is predicted.

At the DFT level, some of the assessed functionals proved to perform within chemical accuracy (±1 kcal/mol ≈ 350 cm^{-1}) for the spin-state energetics of $[Fe(NCH)_6]^{2+}$ (X3LYP, CAM-B3LYP), others for that of $[Co(NCH)_6]^{2+}$ (PBE0, M06, mPW2-PLYP), but none of them did perform so accurately for both complexes at the same time. Only the mPW2-PLYP functional gives for both complexes ΔE^{el}_{HL} values that are within ±2 kcal/mol of the best *ab initio* estimates. For the height Δ_{JT} of the barrier to pseudorotation in LS $[Co(NCH)_6]^{2+}$, remarkably accurate results are obtained with the specialized mPW1K and BB1K "kinetics" functionals and also with the LC-PBE functionals.

Regarding the performances of the functionals for the spin-state energetics of the two complexes, the results obtained with the RSHs suggest that, for such functionals, there is a need for a nonvanishing HF exchange contribution at short-range. This is in line with the fact that the electronic rearrangement accompanying the LS ↔ HS change of states and the concomitant variation of exchange interactions are mainly localized in the compact 3d shell of the TMs. Besides this, no other trend could however be identified within and between the different classes of tested functionals. Still, given the high flexibility of the functional forms, our result makes us believe that it is possible to devise semiempirical functionals, likely of any of the considered types, that perform accurately for TM spin-state energetics.

The CAM-PBE0 functional is the most interesting in this respect. This RSH is characterized by α = 0.25, $\beta = 1 - \alpha$ = 0.75, and ω = 0.30 au^{-1} [eq 19]. It overestimates ΔE^{el}_{HL} for both complexes and gives NR values of the right sign (Table 8). Therefore, increasing the amount of short-range HF exchange in this functional by increasing α or ω could help improve the results for *both* complexes by stabilizing the HS state with respect to the LS state. To probe this proposal, we have calculated with the CAM-PBE0 functional the HS−LS energy difference in the two complexes while varying $\alpha \in [0.15,0.35]$ and $\omega \in [0.10,0.55]$ au^{-1}. The results are summarized in Figure 4 by the plots of the dependence on α and ω of the difference

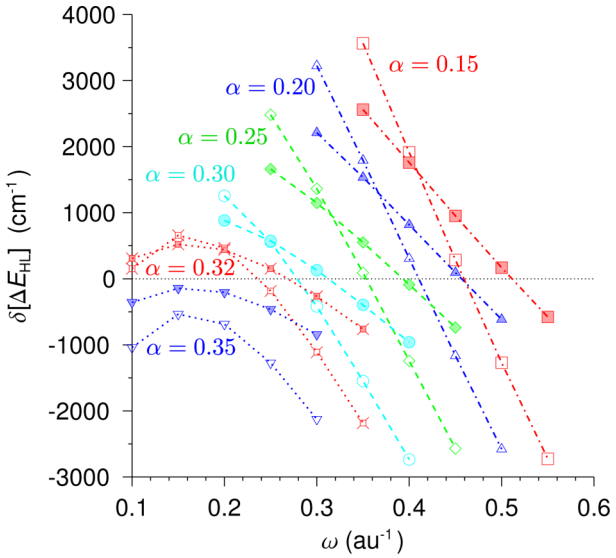

Figure 4. Influence of the fraction α of HF exchange and of the range separation parameter ω on the performance of the range-separated hybrid CAM-PBE0 for the HS−LS energy difference in $[M(NCH)_6]^{2+}$ (M = Fe, Co): plots of the dependence on α and ω of $\delta[\Delta E^{el}_{HL}] = \Delta E^{el}_{HL}|_{\alpha,\omega} - \Delta E^{el}_{HL}|_{CCSD(T)/CBS(\infty)}$ for $[Fe(NCH)_6]^{2+}$ (open symbols) and $[Co(NCH)_6]^{2+}$ (filled symbols).

between the CAM-PBE0 estimate, $\Delta E^{el}_{HL}|_{\alpha,\omega}$, and the best *ab initio* estimate, $\Delta E^{el}_{HL}|_{CCSD(T)/CBS(\infty)}$. We note in Figure 4 that a slight increase of the amount of short-range HF exchange to α = 0.32 accompanied by a slight decrease of the range separation parameter to ω = 0.25 au^{-1} suffices to obtain an RSH which performs within chemical accuracy for the evaluation of ΔE^{el}_{HL} in both complexes at the same time. The reparametrized CAM-PBE0 indeed gives for $[Fe(NCH)_6]^{2+}$ and $[Co(NCH)_6]^{2+}$ NR ΔE^{el}_{HL} values of −2220 cm^{-1} and −3651 cm^{-1}, respectively, the reference ΔE^{el}_{HL} estimates being −2036 cm^{-1} and −3805 cm^{-1}, respectively.

The results of this "CAM-PBE0" exploratory case study are very promising, for they confirm that performing semiempirical functionals of broad applicability may be devised by including in the training sets data relative to TM spin-state energetics.[170] So, to enrich our data set, we are completing the CC characterization of the spin-state energetics of the complexes $[Mn(NCH)_6]^{2+}$, $[Ni(NCH)_6]^{2+}$, $[Fe(NCH)_6]^{3+}$, and $[Co(NCH)_6]^{3+}$ and have started extending the CC study to another class of TM complexes, namely the metalloporphyrins. In the search for a reliable approach to the calculation of spin-state energy differences in TM systems, we will also use these reference data to assess the performance of the NEVPT2 second-order MRPT method.[171−175] The results will be reported in forthcoming papers.

dx.doi.org/10.1021/ct300592w | J. Chem. Theory Comput. 2012, 8, 4216−4231

■ ASSOCIATED CONTENT

Supporting Information

The reference $[M(NCH)_6]^{2+}$ geometries (M = Fe, Co), the results of nonrelativistic frozen-core CC test calculations (HS−LS energy differences in both complexes and barrier height Δ_{JT} for LS $[Co(NCH)_6]^{2+}$), and the results of test calculations performed for assessing the basis set dependency of the DFT results and those of test calculations for the determination of the scalar-relativistic shifts within DFT. The five largest T_1 and T_2 cluster amplitudes obtained in the CCSD/$S^{NR}_{2,Q}$ calculations and the natural orbital occupation numbers in the CASSCF/ANO-II calculations. This material is available free of charge via the Internet at http://pubs.acs.org/.

■ AUTHOR INFORMATION

Corresponding Author

*E-mail: max.lawson@unige.ch.

Notes

The authors declare no competing financial interest.

■ ACKNOWLEDGMENTS

This work was supported by a grant from the Swiss National Supercomputing Centre (CSCS) under project ID s296.

■ REFERENCES

(1) *Spin Crossover in Transition Metal Compounds I*; Gütlich, P., Goodwin, H. A., Eds.; Springer-Verlag: Heidelberg, Germany, 2004.
(2) *Spin Crossover in Transition Metal Compounds II*; Gütlich, P., Goodwin, H. A., Eds.; Springer-Verlag: Heidelberg, Germany, 2004.
(3) *Spin Crossover in Transition Metal Compounds III*; Gütlich, P., Goodwin, H. A., Eds.; Springer-Verlag: Heidelberg, Germany, 2004.
(4) Ghosh, A.; Taylor, P. R. *Curr. Opin. Chem. Biol.* **2003**, *7*, 113−124.
(5) Harvey, J. N.; Poli, R.; Smith, K. M. *Coord. Chem. Rev.* **2003**, *238*−*239*, 347−361.
(6) Shaik, S.; Cohen, S.; Wang, Y.; Chen, H.; Kumar, D.; Thiel, W. *Chem. Rev.* **2010**, *110*, 949−1017.
(7) Hohenberg, P.; Kohn, W. *Phys. Rev.* **1964**, *136*, B864−B871.
(8) Kohn, W.; Sham, L. J. *Phys. Rev.* **1965**, *140*, A1133−A1138.
(9) Bolvin, A. J. *Phys. Chem. A* **1998**, *102*, 7525−7534.
(10) Paulsen, H.; Duelund, L.; Winkler, H.; Toftlund, H.; Trautwein, A. X. *Inorg. Chem.* **2001**, *40*, 2201−2204.
(11) Reiher, M.; Salomon, O.; Hess, B. A. *Theor. Chem. Acc.* **2001**, *107*, 48−55.
(12) Salomon, O.; Reiher, M.; Hess, B. A. *J. Chem. Phys.* **2002**, *117*, 4729−4737.
(13) Fouqueau, A.; Mer, S.; Casida, M. E.; Lawson Daku, L. M.; Hauser, A.; Mineva, T. *J. Chem. Phys.* **2004**, *120*, 9473−9486.
(14) Deeth, R. J.; Fey, N. *J. Comput. Chem.* **2004**, *25*, 1840−1848.
(15) Paulsen, H.; Trautwein, A. X. In *Spin Crossover in Transition Metal Compounds II*; Gütlich, P., Goodwin, H. A., Eds.; Springer-Verlag: Heidelberg, Germany, 2004; Top. Curr. Chem., Vol. *235*; pp 197−219.
(16) Kaltsoyannis, N.;McGrady, J.; Harvey, J. *Principles and Applications of Density Functional Theory in Inorganic Chemistry I*; Springer: Berlin/Heidelberg, 2004; Structure & Bonding, Vol. *112*; pp 81−102.
(17) Swart, M.; Groenhof, A. R.; Ehlers, A. W.; Lammertsma, K. *J. Phys. Chem. A* **2004**, *108*, 5479−5483.
(18) Ganzenmüller, G.; Berkaïne, N.; Fouqueau, A.; Casida, M. E.; Reiher, M. *J. Chem. Phys.* **2005**, *122*, 234321.
(19) Smith, D. M. A.; Dupuis, M.; Straatsma, T. P. *Mol. Phys.* **2005**, *103*, 273−278.
(20) Lawson Daku, L. M.; Vargas, A.; Hauser, A.; Fouqueau, A.; Casida, M. E. *ChemPhysChem* **2005**, *6*, 1393−1410.
(21) Fouqueau, A.; Casida, M. E.; Lawson Daku, L. M.; Hauser, A.; Neese, F. *J. Chem. Phys.* **2005**, *122*, 044110.
(22) Ghosh, A. *J. Biol. Inorg. Chem.* **2006**, *11*, 712−724.
(23) Vargas, A.; Zerara, M.; Krausz, E.; Hauser, A.; Lawson Daku, L. M. *J. Chem. Theory Comput.* **2006**, *2*, 1342−1359.
(24) Hauser, A.; Enachescu, C.; Lawson Daku, M.; Vargas, A.; Amstutz, N. *Coord. Chem. Rev.* **2006**, *250*, 1642−1652.
(25) Scherlis, D. A.; Cococcioni, M.; Sit, P.; Marzari, N. *J. Phys. Chem. B* **2007**, *111*, 7384−7391.
(26) Guillon, T.; Salmon, L.; Molnár, G.; Zein, S.; Borshch, S.; Bousseksou, A. *J. Phys. Chem. A* **2007**, *111*, 8223−8228.
(27) Zein, S.; Borshch, S. A.; Fleurat-Lessard, P.; Casida, M. E.; Chermette, H. *J. Chem. Phys.* **2007**, *126*, 014105.
(28) Tangen, E.; Conradie, J.; Ghosh, A. *J. Chem. Theory Comput.* **2007**, *3*, 448−457.
(29) Conradie, J.; Ghosh, A. *J. Chem. Theory Comput.* **2007**, *3*, 689−702.
(30) Wasbotten, I. H.; Ghosh, A. *Inorg. Chem.* **2007**, *46*, 7890−7898.
(31) Conradie, J.; Wondimagegn, T.; Ghosh, A. *J. Phys. Chem. B* **2008**, *112*, 1053−1056.
(32) Pierloot, K.; Vancoillie, S. *J. Chem. Phys.* **2008**, *128*, 034104.
(33) Marti, K. H.; Ondík, I. M.; Moritz, G.; Reiher, M. *J. Chem. Phys.* **2008**, *128*, 014104.
(34) Jensen, K. P. *Inorg. Chem.* **2008**, *47*, 10357−10365.
(35) Swart, M. *J. Chem. Theory Comput.* **2008**, *4*, 2057−2066.
(36) Rotzinger, F. P. *J. Chem. Theory Comput.* **2009**, *5*, 1061−1067.
(37) Jensen, K. P.; Cirera, J. *J. Phys. Chem. A* **2009**, *113*, 10033−10039.
(38) Vargas, A.; Hauser, A.; Lawson Daku, L. M. *J. Chem. Theory Comput.* **2009**, *5*, 97−115.
(39) Oláh, J.; Harvey, J. N. *J. Phys. Chem. A* **2009**, *113*, 7338−7345.
(40) Lawson Daku, L. M.; Hauser, A. *J. Phys. Chem. Lett.* **2010**, *1*, 1830−1835.
(41) Ye, S.; Neese, F. *Inorg. Chem.* **2010**, *49*, 772−774.
(42) Zhao, H.; Pierloot, K.; Langner, E. H. G.; Swarts, J. C.; Conradie, J.; Ghosh, A. *Inorg. Chem.* **2012**, *51*, 4002−4006.
(43) Andersson, K.; Malmqvist, P.-A.; Roos, B. O.; Sadlej, A. J.; Wolinski, K. *J. Phys. Chem.* **1990**, *94*, 5483−5488.
(44) Andersson, K.; Malmqvist, P.-A.; Roos, B. O. *J. Chem. Phys.* **1992**, *96*, 1218−1226.
(45) Ghigo, G.; Roos, B. O.; Malmqvist, P.-A. *Chem. Phys. Lett.* **2004**, *396*, 142−149.
(46) Kepenekian, M.; Robert, V.; Le Guennic, B. *J. Chem. Phys.* **2009**, *131*, 114702.
(47) Vancoillie, S.; Zhao, H.; Radoń, M.; Pierloot, K. *J. Chem. Theory Comput.* **2010**, *6*, 576−582.
(48) Bartlett, R. J.; Musiał, M. *Rev. Mod. Phys.* **2007**, *79*, 291−352.
(49) Krylov, A. I. *Annu. Rev. Phys. Chem.* **2008**, *59*, 433−462.
(50) Kowalski, K.; Valiev, M. *J. Chem. Phys.* **2009**, *131*, 234107.
(51) Gütlich, P.; Hauser, A.; Spiering, H. *Angew. Chem., Int. Ed. Engl.* **1994**, *33*, 2024−2054.
(52) Hauser, A.; Amstutz, N.; Delahaye, S.; Sadki, A.; Schenker, S.; Sieber, R.; Zerara, M. *Struct. Bonding (Berlin)* **2004**, *106*, 81−96.
(53) The HS−LS Gibbs free-energy difference associated with the LS ⇆ HS equilibrium in an SCO compound reads $\Delta G_{HL}(T,P) = -RT \log[\gamma_{HS}/(1 - \gamma_{HS})]$, where $\gamma_{HS}(T,P)$ is the HS fraction which can be determined from spectroscopic or magnetization measurements. The HS−LS enthaphy difference is obtained from the experimental spin-transition curve $\gamma_{HS} = \gamma_{HS}(T,P)$ by using the relation $\Delta H_{HL}(T,P) = \Delta G_{HL}(T,P) - T[(\partial \Delta G_{HL}/\partial T)_P]$. The usually reported ΔH_{HL} values are for the ambient pressure and the transition temperature $T_{1/2}$, which is the temperature at which $\gamma_{HS} = 1/2$.
(54) Vargas, A.; Krivokapic, I.; Hauser, A.; Lawson Daku, L. M. To be published.
(55) Constant, G.; Daran, J. C.; Jeannin, Y. *J. Solid State Chem.* **1970**, *2*, 421−429.
(56) Constant, G.; Daran, J. C.; Jeannin, Y. *J. Inorg. Nucl. Chem.* **1973**, *35*, 4093−4102.

(57) Raghavachari, K.; Trucks, G. W.; Pople, J. A.; Head-Gordon, M. *Chem. Phys. Lett.* **1989**, *157*, 479−483.
(58) Perdew, J. P.; Burke, K.; Ernzerhof, M. *Phys. Rev. Lett.* **1996**, *77*, 3865−3868.
(59) Perdew, J. P.; Burke, K.; Ernzerhof, M. *Phys. Rev. Lett.* **1997**, *78*, 1396.
(60) Becke, A. D. *J. Chem. Phys.* **1993**, *98*, 5648−5652.
(61) Becke3LYP Method References and General Citation Guidelines. *Gaussian NEWS*, **1994** (summer), *5* (2), 2.
(62) Becke, A. D. *Phys. Rev. A* **1988**, *38*, 3098−3100.
(63) Lee, C.; Yang, W.; Parr, R. G. *Phys. Rev. B* **1988**, *37*, 785−789.
(64) Perdew, J. P. *Phys. Rev. B* **1986**, *33*, 8822−8824.
(65) Perdew, J. P. *Phys. Rev. B* **1986**, *34*, 7406.
(66) Xu, X.; Goddard, W. A., III. *Proc. Natl. Acad. Sci. U. S. A.* **2004**, *101*, 2673−2677.
(67) Tsuneda, T.; Suzumura, T.; Hirao, K. *J. Chem. Phys.* **1999**, *110*, 10664−10678.
(68) Perdew, J. P.; Ernzerhof, M.; Burke, K. *J. Chem. Phys.* **1996**, *105*, 9982−9985.
(69) Adamo, C.; Barone, V. *J. Chem. Phys.* **1999**, *110*, 6158−6170.
(70) Becke, A. D. *J. Chem. Phys.* **1997**, *107*, 8554−8560.
(71) Handy, N. C.; Cohen, A. *J. Mol. Phys.* **2001**, *99*, 403−412.
(72) Keal, T. W.; Tozer, D. J. *J. Chem. Phys.* **2005**, *123*, 121103.
(73) Schmider, H. L.; Becke, A. D. *J. Chem. Phys.* **1998**, *108*, 9624−9631.
(74) Boese, A. D.; Handy, N. C. *J. Chem. Phys.* **2001**, *114*, 5497−5503.
(75) Lynch, B. J.; Fast, P. L.; Harris, M.; Truhlar, D. G. *J. Phys. Chem. A* **2000**, *104*, 4811−4815.
(76) Boese, A. D.; Chandra, A.; Martin, J.M. L.; Marx, D. *J. Chem. Phys.* **2003**, *119*, 5965−5980.
(77) Tao, J.; Perdew, J. P.; Staroverov, V. N.; Scuseria, G. E. *Phys. Rev. Lett.* **2003**, *91*, 146401.
(78) Zhao, Y.; Lynch, B. J.; Truhlar, D. G. *J. Phys. Chem. A* **2004**, *108*, 2715−2719.
(79) Perdew, J. P.; Kurth, S.; Zupan, A.; Blaha, P. *Phys. Rev. Lett.* **1999**, *82*, 2544−2547.
(80) Perdew, J. P.; Kurth, S.; Zupan, A.; Blaha, P. *Phys. Rev. Lett.* **1999**, *82*, 5179.
(81) Staroverov, V. N.; Scuseria, G. E.; Tao, J.; Perdew, J. P. *J. Chem. Phys.* **2003**, *119*, 12129−12137.
(82) Zhao, Y.; Truhlar, D. G. *J. Chem. Phys.* **2006**, *125*, 194101.
(83) Zhao, Y.; Schultz, N. E.; Truhlar, D. G. *J. Chem. Phys.* **2005**, *123*, 161103.
(84) Zhao, Y.; Schultz, N. E.; Truhlar, D. G. *J. Chem. Theory Comput.* **2006**, *2*, 364−382.
(85) Zhao, Y.; Truhlar, D. G. *Theor. Chem. Acc.* **2008**, *120*, 215−241.
(86) Yanai, T.; Tew, D. P.; Handy, N. C. *Chem. Phys. Lett.* **2004**, *393*, 51−57.
(87) Grimme, S. *J. Chem. Phys.* **2006**, *124*, 034108.
(88) Schwabe, T.; Grimme, S. *Phys. Chem. Chem. Phys.* **2007**, *8*, 4398−4401.
(89) Iikura, H.; Tsuneda, T.; Yanai, T.; Hirao, K. *J. Chem. Phys.* **2001**, *115*, 3540−3544.
(90) Tawada, Y.; Tsuneda, T.; Yanagisawa, S.; Yanai, T.; Hirao, K. *J. Chem. Phys.* **2004**, *120*, 8425−8433.
(91) Rohrdanz, M. A.; Herbert, J. M. *J. Chem. Phys.* **2008**, *129*, 034107.
(92) Fonseca Guerra, C.; Snijders, J.; te Velde, G.; Baerends, E. J. *Theor. Chem. Acc.* **1998**, *99*, 391−403.
(93) te Velde, G.; Bickelhaupt, F. M.; Baerends, E. J.; Fonseca Guerra, C.; van Gisbergen, S. J. A.; Snijders, J. G.; Ziegler, T. *J. Comput. Chem.* **2001**, *22*, 931−967.
(94) Baerends, E. J.; Ziegler, T.; Autschbach, J.; Bashford, D.; Bérces, A.; Bickelhaupt, F. M.; Bo, C.; Boerrigter, P. M.; Cavallo, L.; Chong, D. P.; Deng, L.; Dickson, R. M.; Ellis, D. E.; van Faassen, M.; Fan, L.; Fischer, T. H.; Guerra, C. F.; Ghysels, A.; Giammona, A.; van Gisbergen, S. J. A.; Götz, A.; Groeneveld, J.; Gritsenko, O. V.; Groening, M.; Gusarov, S.; Harris, F. E.; van den Hoek, P.; Jacob, C. R.; Jacobsen, H.; Jensen, L.; Kaminski, J. W.; van Kessel, G.; Kootstra, F.; Kovalenko, A.; Krykunov, M. V.; van Lenthe, E.; McCormack, D. A.; Michalak, A.; Mitoraj, M.; Neugebauer, J.; Nicu, V. P.; Noodleman, L.; Osinga, V. P.; Patchkovskii, S.; Philipsen, P. H. T.; Post, D.; Pye, C. C.; Ravenek, W.; Rodríguez, J. I.; Ros, P.; Schipper, P. R. T.; Schreckenbach, G.; Seldenthuis, J.; Seth, M.; Snijders, J. G.; Solá, M.; Swart, M.; Swerhone, D.; te Velde, G.; Vernooijs, P.; Versluis, L.; Visscher, L.; Visser, O.; Wang, F.; Wesolowski, T. A.; van Wezenbeek, E. M.; Wiesenekker, G.; Wolff, S. K.; Woo, T. K.; Yakovlev, A. L. *ADF2009, SCM*; Theoretical Chemistry, Vrije Universiteit: Amsterdam, The Netherlands. http://www.scm.com (accessed August 20, 2012).
(95) Van Lenthe, E.; Baerends, E. J. *J. Comput. Chem.* **2003**, *24*, 1142−1156.
(96) Hirata, S. *J. Phys. Chem. A* **2003**, *107*, 9887−9897.
(97) Hirata, S.; Fan, P.-D.; Auer, A. A.; Nooijen, M.; Piecuch, P. *J. Chem. Phys.* **2004**, *121*, 12197−12207.
(98) Hirata, S.; Yanai, T.; Harrison, R. J.; Kamiya, M.; Fan, P.-D. *J. Chem. Phys.* **2007**, *126*, 024104.
(99) Valiev, M.; Bylaska, E.; Govind, N.; Kowalski, K.; Straatsma, T. P.; Van Dam, H. J. J.; Wang, D.; Nieplocha, J.; Apra, E.; Windus, T. L.; de Jong, W. A. *Comput. Phys. Commun.* **2010**, *181*, 1477−1489.
(100) de Jong, W. A.; Bylaska, E.; Govind, N.; Janssen, C. L.; Kowalski, K.; Müller, T.; Nielsen, I. M. B.; van Dam, H. J. J.; Veryazov, V.; Lindh, R. *Phys. Chem. Chem. Phys.* **2010**, *12*, 6896−6920.
(101) Douglas, M.; Kroll, N. M. *Ann. Phys.* **1974**, *82*, 89−155.
(102) Hess, B. A. *Phys. Rev. A* **1985**, *32*, 756−763.
(103) Hess, B. A. *Phys. Rev. A* **1986**, *33*, 3742−3748.
(104) de Jong, W. A.; Harrison, R. J.; Dixon, D. A. *J. Chem. Phys.* **2001**, *114*, 48−53.
(105) Dunning, T. H., Jr. *J. Chem. Phys.* **1989**, *90*, 1007−1023.
(106) Balabanov, N. B.; Peterson, K. A. *J. Chem. Phys.* **2005**, *123*, 064107.
(107) Helgaker, T.; Klopper, W.; Koch, H.; Noga, J. *J. Chem. Phys.* **1997**, *106*, 9639−9646.
(108) Peterson, K. A.; Woon, D. E.; Dunning, T. H., Jr. *J. Chem. Phys.* **1994**, *100*, 7410.
(109) Malmqvist, P.-A.; Rendell, A.; Roos, B. O. *J. Phys. Chem.* **1990**, *94*, 5477−5482.
(110) Aquilante, F.; Pedersen, T. B.; Lindh, R.; Roos, B. O.; de Merás, A. S.; Koch, H. *J. Chem. Phys.* **2008**, *129*, 024113.
(111) Aquilante, F.; Malmqvist, P.-A.; Pedersen, T. B.; Ghosh, A.; Roos, B. O. *J. Chem. Theory Comput.* **2008**, *4*, 694−702.
(112) Roca-Sanjuán, D.; Aquilante, F.; Lindh, R. *WIREs Comput. Mol. Sci.* **2012**, *2*, 585−603.
(113) Aquilante, F.; De Vico, L.; Ferré, N.; Ghigo, G.; Malmqvist, P.-Å.; Neogrády, P.; Pedersen, T. B.; Pitoňák, M.; Reiher, M.; Roos, B. O.; Serrano-Andrés, L.; Urban, M.; Veryazov, V.; Lindh, R. *J. Comput. Chem.* **2010**, *31*, 224−247.
(114) Veryazov, V.; Widmark, P.-O.; Serrano-Andrés, L.; Lindh, R.; Roos, B. O. *Int. J. Quantum Chem.* **2004**, *100*, 626−635.
(115) Karlström, G.; Lindh, R.; Malmqvist, P.-Å.; Roos, B. O.; Ryde, U.; Veryazov, V.; Widmark, P.-O.; Cossi, M.; Schimmelpfennig, B.; Neogrady, P.; Seijo, L. *Comput. Mater. Sci.* **2003**, *28*, 222−239.
(116) Roos, B. O.; Lindh, R.; Malmqvist, P.-A.; Veryazov, V.; Widmark, P.-O. *J. Phys. Chem. A* **2005**, *109*, 6575−6579.
(117) Roos, B. O.; Lindh, R.; Malmqvist, P.-A.; Veryazov, V.; Widmark, P.-O. *J. Phys. Chem. A* **2004**, *108*, 2851−2858.
(118) Pierloot, K.; Dumez, B.; Widmark, P.-O.; Roos, B. O. *Theor. Chem. Acc.* **1995**, *90*, 87−114.
(119) Boström, J.; Delcey, M. G.; Aquilante, F.; Serrano-Andrés, L.; Pedersen, T. B.; Lindh, R. *J. Chem. Theory Comput.* **2010**, *6*, 747−754.
(120) Forsberg, N.; Malmqvist, P.-A. *Chem. Phys. Lett.* **1997**, *274*, 196−204.
(121) Andersson, K.; Roos, B. O. *Chem. Phys. Lett.* **1992**, *191*, 507−514.
(122) Pierloot, K. In *Computational Organometallic Chemistry*; Cundari, T., Ed.; Marcel Dekker, Inc.: New York, 2001; pp 123−158.

(123) Bersuker, I. B. *The Jahn-Teller Effect*; Cambridge University Press: Cambridge, U. K., 2006; pp 45−109.
(124) Bersuker, I. B. *The Jahn-Teller Effect*; Cambridge University Press: Cambridge, U. K., 2006; pp 162−262.
(125) Sax, A. F. *Chem. Phys.* **2008**, *349*, 9−31.
(126) Beste, A.; Bartlett, R. J. *Chem. Phys. Lett.* **2002**, *366*, 100−108.
(127) Jiang, W.; DeYonker, N. J.; Wilson, A. K. *J. Chem. Theory Comput.* **2012**, *8*, 460−468.
(128) Lee, T. J.; Taylor, P. R. *Int. J. Quantum Chem.* **1989**, *36*, 199−207.
(129) Lee, T. J.; Rice, J. E.; Scuseria, G. E.; Schaefer, H. F. *Theor. Chim. Acta* **1989**, *75*, 81−98.
(130) Leininger, M. L.; Nielsen, I. M.; Crawford, T.; Janssen, C. L. *Chem. Phys. Lett.* **2000**, *328*, 431−436.
(131) Lee, T. J. *Chem. Phys. Lett.* **2003**, *372*, 362−367.
(132) Karton, A.; Rabinovich, E.; Martin, J. M. L.; Ruscic, B. *J. Chem. Phys.* **2006**, *125*, 144108.
(133) Karton, A.; Daon, S.; Martin, J. M. *Chem. Phys. Lett.* **2011**, *510*, 165−178.
(134) Andersson, K.; Roos, B. O. *Int. J. Quantum Chem.* **1993**, *45*, 591−607.
(135) Roos, B. O.; Andersson, K.; Fülscher, M. P.; Malmqvist, P.-a.; Serrano-Andrés, L.; Pierloot, K.; Merchán, M. *Adv. Chem. Phys.* **2007**, *93*, 219−331.
(136) Andersson, K. *Theor. Chim. Acta* **1995**, *91*, 31−46.
(137) Kepenekian, M.; Robert, V.; Le Guennic, B.; De Graaf, C. *J. Comput. Chem.* **2009**, *30*, 2327−2333.
(138) Suaud, N.; Bonnet, M.-L.; Boilleau, C.; Labèguerie, P.; Guihéry, N. *J. Am. Chem. Soc.* **2009**, *131*, 715−722.
(139) Schmidt, M. W.; Gordon, M. S. *Annu. Rev. Phys. Chem.* **1998**, *49*, 233−266.
(140) Ceperley, D. M.; Adler, B. J. *Phys. Rev. Lett.* **1980**, *45*, 566−569.
(141) Vosko, S. H.; Wilk, L.; Nusair, M. *Can. J. Phys.* **1980**, *58*, 1200−1211.
(142) Wang, Y.; Perdew, J. P. *Phys. Rev. B* **1991**, *44*, 13298−13307.
(143) Perdew, J. P.; Wang, Y. *Phys. Rev. B* **1992**, *45*, 13244−13249.
(144) Dirac, P. A. M. *Proc. R. Soc. London, Ser. A* **1929**, *123*, 714−733.
(145) Slater, J. C. *Phys. Rev.* **1951**, *81*, 385−390.
(146) Jones, R. O.; Gunnarsson, O. *Rev. Mod. Phys.* **1989**, *61*, 689−746.
(147) Dreizler, R. M.; Gross, E. K. U. *Density Functional Theory, An Approach to the Quantum Many-Body Problem*; Springer-Verlag: New York, 1990; pp 173−244.
(148) Ma, S.-K.; Brueckner, K. E. *Phys. Rev.* **1968**, *165*, 18−31.
(149) Langreth, D. C.; Mehl, M. J. *Phys. Rev. B* **1983**, *28*, 1809−1834.
(150) Langreth, D. C.; Mehl, M. J. *Phys. Rev. B* **1984**, *29*, 2310.
(151) Nekovee, M.; Foulkes, W. M. C. *J. Phys. Rev. Lett.* **2001**, *87*, 036401.
(152) Perdew, J. P.; Tao, J.; Staroverov, V. N.; Scuseria, G. E. *J. Chem. Phys.* **2004**, *120*, 6898−6911.
(153) Harris, J.; Jones, R. O. *J. Phys. F: Met. Phys.* **1974**, *4*, 1170−1186.
(154) Langreth, D. C.; Perdew, J. P. *Solid State Commun.* **1975**, *17*, 1425−1429.
(155) Gunnarsson, O.; Lundqvist, B. I. *Phys. Rev. B* **1976**, *13*, 4274−4298.
(156) Gunnarsson, O.; Lundqvist, B. I. *Phys. Rev. B* **1977**, *15*, 6006.
(157) Langreth, D. C.; Perdew, J. P. *Phys. Rev. B* **1977**, *15*, 2884−2901.
(158) Harris, J. *Phys. Rev. A* **1984**, *29*, 1648−1659.
(159) Becke, A. D. *J. Chem. Phys.* **1993**, *98*, 1372−1377.
(160) Savin, A. In *Recent Advances in Density Functional Methods (Part I)*; Chong, D. P., Ed.; World Scientific Publishing Company: River Edge, NJ, 1995; Recent Advances In Computational Chemistry, Vol. *1*; pp 129−153.
(161) Leininger, T.; Stoll, H.; Werner, H.-J.; Savin, A. *Chem. Phys. Lett.* **1997**, *275*, 151−160.
(162) Toulouse, J.; Colonna, F.; Savin, A. *Phys. Rev. A* **2004**, *70*, 062505.
(163) Song, J.-W.; Hirosawa, T.; Tsuneda, T.; Hirao, K. *J. Chem. Phys.* **2007**, *126*, 154105.
(164) Görling, A.; Levy, M. *Phys. Rev. B* **1993**, *47*, 13105−13113.
(165) Görling, A.; Levy, M. *Phys. Rev. A* **1994**, *50*, 196−204.
(166) Schwabe, T.; Grimme, S. *Acc. Chem. Res.* **2008**, *41*, 569−579.
(167) Perdew, J. P.; Schmidt, K. *AIP Conf. Proc.* **2001**, *577*, 1−20.
(168) Schenk, G.; Pau, M. Y. M.; Solomon, E. I. *J. Am. Chem. Soc.* **2004**, *126*, 505−515.
(169) Adamo, C.; Barone, V. *J. Chem. Phys.* **1998**, *108*, 664−675.
(170) Note that the reparametrization of the CAM-PBE0 functional ($\alpha = 0.32$, $\beta = 0.68$, $\omega = 0.25$ au^{-1}) did not lead to an improvement of the result obtained for the barrier height Δ_{JT}: while the original CAM-PBE0 functional gives $\Delta_{JT} = 153$ cm^{-1}, a value of 107 cm^{-1} is now obtained, the best Δ_{JT} estimate being 273 cm^{-1}. Actually, the results obtained with the LC-PBE RSH show that, with the CAM-PBE0 functional form, the requirement on the amount of HF exchange at short-range for the determination of Δ_{JT} differs from the one associated with the evaluation of Δ_{HL}^{el}. The LC-PBE functional, which performs exceptionally well for the determination of Δ_{JT} ($\Delta_{JT} = 280$ cm^{-1}), is indeed obtained from the CAM-PBE0 functional form by setting $\alpha = 0$, $\alpha = 1$, and $\omega = 0.30$ au^{-1}.
(171) Angeli, C.; Cimiraglia, R.; Evangelisti, S.; Leininger, T.; Malrieu, J.-P. *J. Chem. Phys.* **2001**, *114*, 10252−10264.
(172) Angeli, C.; Cimiraglia, R.; Malrieu, J.-P. *Chem. Phys. Lett.* **2001**, *350*, 297−305.
(173) Angeli, C.; Cimiraglia, R.; Malrieu, J.-P. *J. Chem. Phys.* **2002**, *117*, 9138−9153.
(174) Angeli, C.; Borini, S.; Cestari, M.; Cimiraglia, R. *J. Chem. Phys.* **2004**, *121*, 4043−4049.
(175) Angeli, C.; Pastore, M.; Cimiraglia, R. *Theor. Chem. Acc.* **2007**, *117*, 743−754.